Recent Progress in Many-Body Theories, Barcelona, Spain, July 16-20, 2007

RPMBT14

Microscopic Studies of the Ground State of solid ^{4}He with Path Integral Projector Monte Carlo

D.E. Galli

Dipartimento di Fisica,
Università degli Studi di Milano

Coworkers

Luciano Reatto

Maurizio Rossi

Ettore Vitali

Riccardo Rota

Filippo Tramonto

Sede centrale: facciata lungo largo Richini

Sede centrale: cortile del Richini

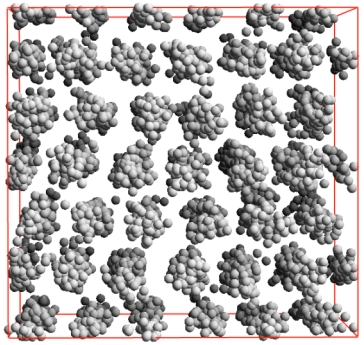

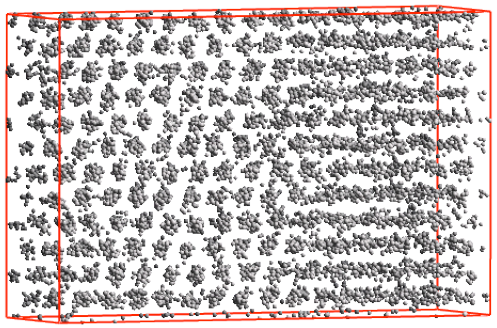

Outline

- Introduction: supersolid, some basic questions for many body theory
- Some special properties of solid ^{4}He
  - Zero point motion
  - Vacancy-interstitial pairs
  - Vacancy waves
- Microscopic theories: T=0 K and T>0 K methods
  - Points of agreement, points of disagreement
- Theoretical tools at T=0 K
  - Variational Shadow Wave Function (SWF)
  - "exact" Shadow Path Integral Ground State (SPIGS)
- One-body density matrix:
  - Study of ODLRO in a commensurate crystal
    - Variational result (SWF)
    - Exact result in 3D and 2D (SPIGS)
  - Study of ODLRO in a crystal with vacancies (incommensurate crystal)
    - Variational result (SWF)
    - "Exact" result (SPIGS)
- Multiple vacancies: stable or unstable?
- Ground state: commensurate or incommensurate?
  - Variational results for concentration of ground state vacancies
- ODLRO at grain boundaries
- Conclusions

SUPERSOLID STATE

A quantum solid (^{4}He) with some sort of superfluid properties like non classical moment of inertia, BEC

Theoretical works ante Kim-Chan experiments (2004)

A. Possible presence of vacancies in the ground state (Andreev and Lifshitz 1969)

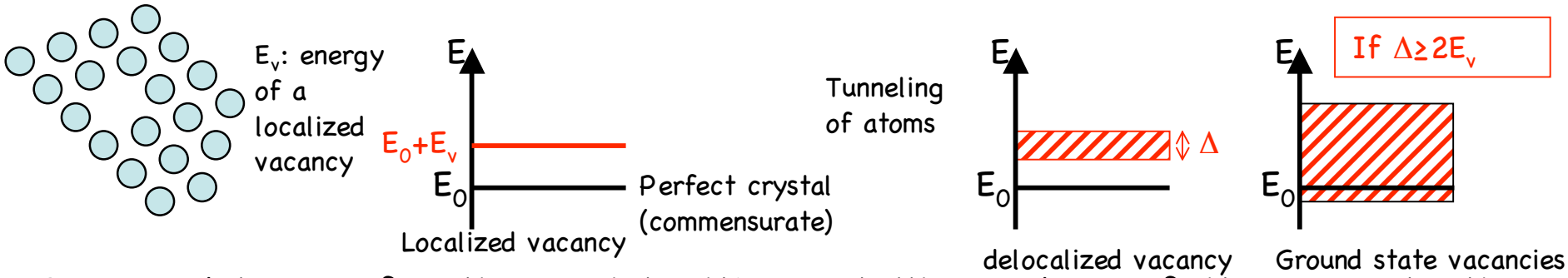

B. Model wave functions exist with crystalline order, a finite concentration of vacancies and a finite BEC
(Chester 1970, stimulated by proof (Reatto 1969) that a Jastrow wf has BEC)

C. Non classical rotation of a quantum solid;
rigidity of wave function: $\rho_s/\rho>0$ if local density $\rho(r)>0$ (Leggett 1970)

D. ...work by Saslow, Guyer,...

....

M. proof that a SWF wf has BEC (Reatto, Masserini, PRB 1988)

....

Z. Microscopic computation of the condensate induced by vacancies in solid ^{4}He from variational theory (Galli-Reatto, JLTP 2001)

Supersolid State

- If Off Diagonal Long Range Order (ODLRO) is present we expect some superfluid phenomena

State with LRO+ODLRO

Behavior of the

one-body density matrix

$$\rho^{(1)}(\vec{r}',\vec{r}) = \left\langle \hat{\Psi}^{+}(\vec{r}')\hat{\Psi}(\vec{r}) \right\rangle$$

$\rho^{(1)}(\vec{r},\vec{r})$ = Local density at $\vec{r}$

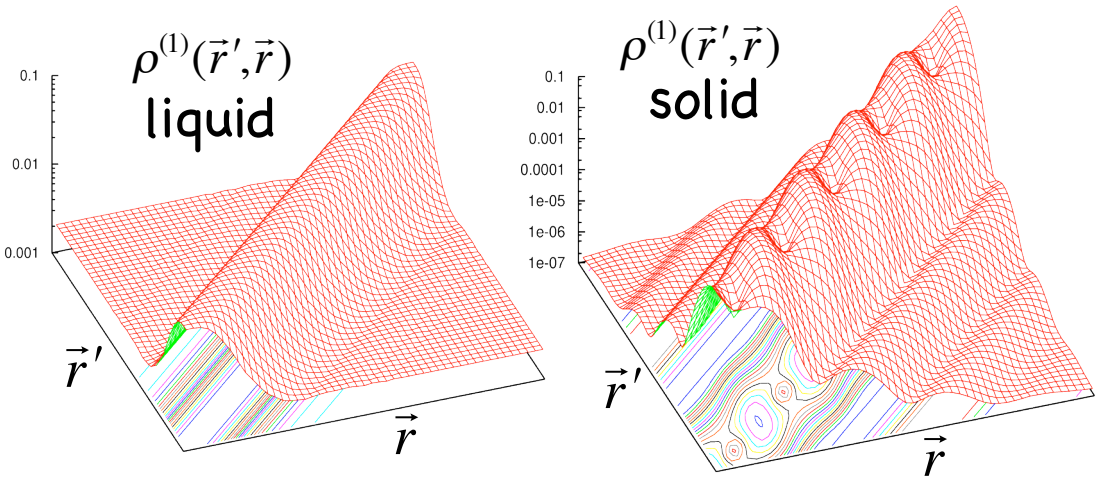

- Theory indicates that this must happen somewhere

(use a Jastrow or a SWF, which both have LRO+ODLRO, to define $\hat{H}$)

- There is now solid evidence that Bose Hubbard model on a lattice can show LRO+ODLRO, in ^{4}He however the lattice is self-built by the atoms

Experiments (1)

- Experimental search of the supersolid state in '70 and '80 has been unsuccessful

BREAKTHROUGH

Kim and Chan find non classical rotational inertia (NCRI) in

- ^{4}He in vycor (Nature, Jan. 2004)
- ^{4}He in porous gold (JLTP, Febr. 2005)
- ^{4}He bulk (Science, Sept. 2004)

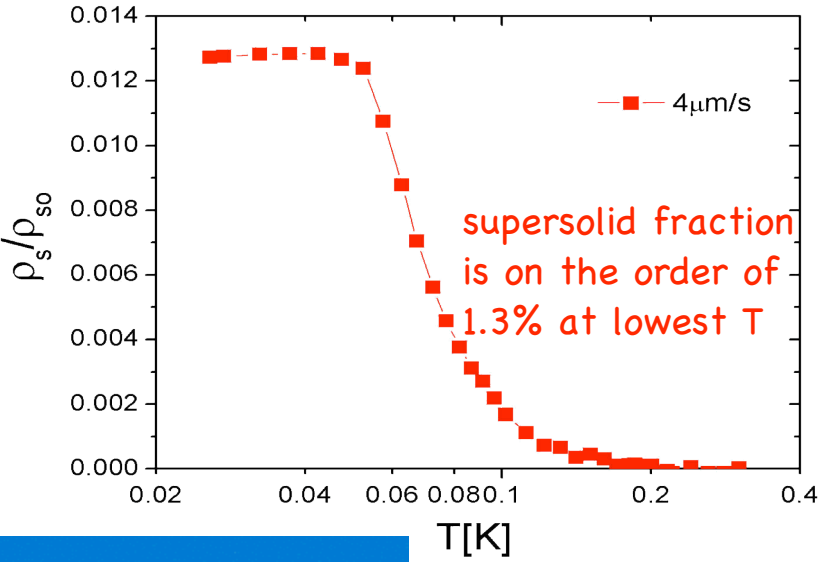

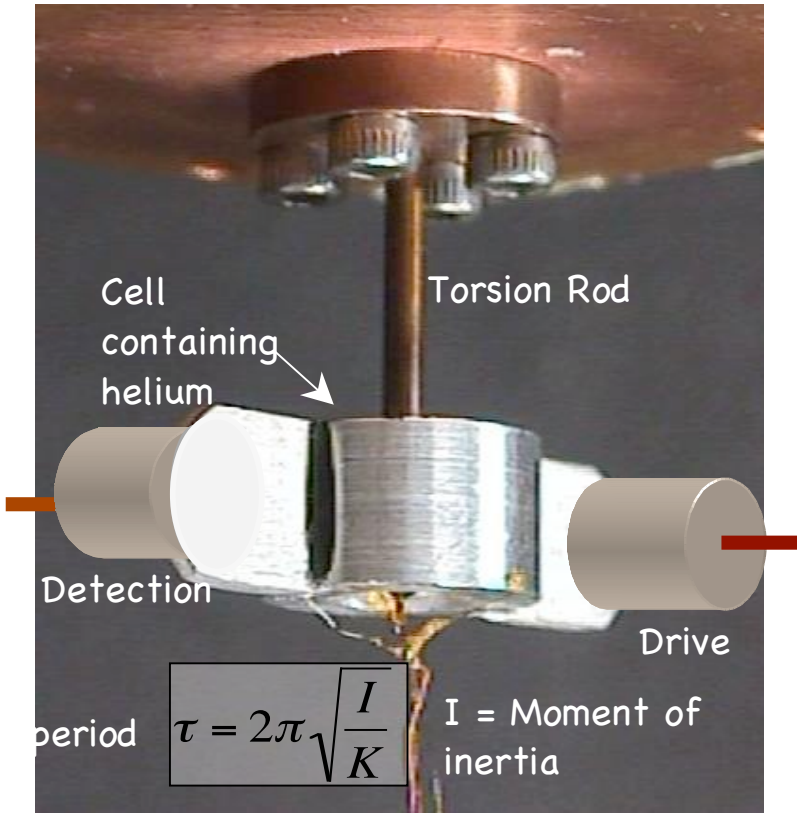

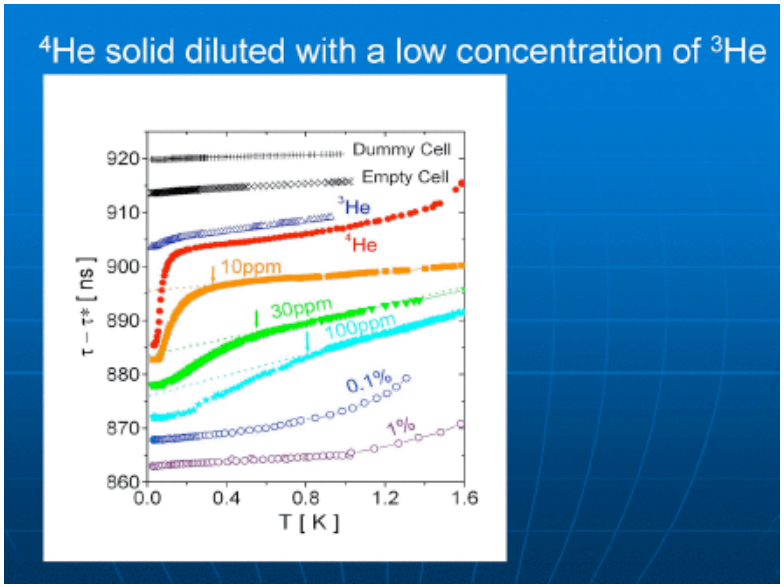

- Superfluidity of bulk crystalline ^{4}He is the correct explanation?

Experiments (2)

Supersolid behavior in torsional oscillator experiments in other laboratories (results reported at workshop "Physics of supersolid and related topics", Keio University, April 2007)

- Rittner-Reppy (Cornell) find NCRI, signal goes below detection level after suitable annealing, in bad quality samples ρ_s/ρ as large as 20% is found
- Shirahama and collaborators (Keio Un.) find NCRI, ρs is one order of magnitude smaller compared to the PSU results
- Penzeyv and Kubota (ISSP, Un. Tokyo) find NCRI for a solid under DC rotation , no dependence on the angular velocity
- Kojima (Rutgers) find NCRI , measurements on the same sample at two different frequencies: results in disagreement with classical glass model (Nussinov)

Other measurements

- Beamish and coworkers experiment (PRL 2005 and 2006) rules out some possible alternative explanations, on the other hand they see no pressure-induced flow in the pores
- Balibar and coworkers (Science 2006) find superflow in solid ^{4}He at coexistence with liquid only when grain boundaries are present, it seems likely that this phenomenon is distinct from the NCRI

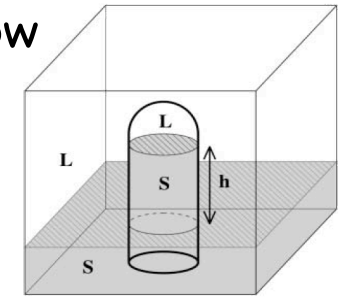

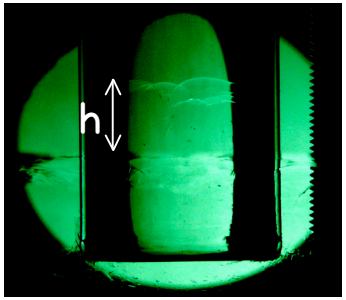

Experiments (3)

Clark, West, Chan, arXiv:0706.0906

- Chan and coworkers find NCRI in a single crystal sample, sharper transition is found but different samples give different ρ_s
- T-dependence in pure ($x_{3He} \approx 10^{-9}$) samples collapses into a single curve which can be fitted with 2/3 power law (3D XY model)

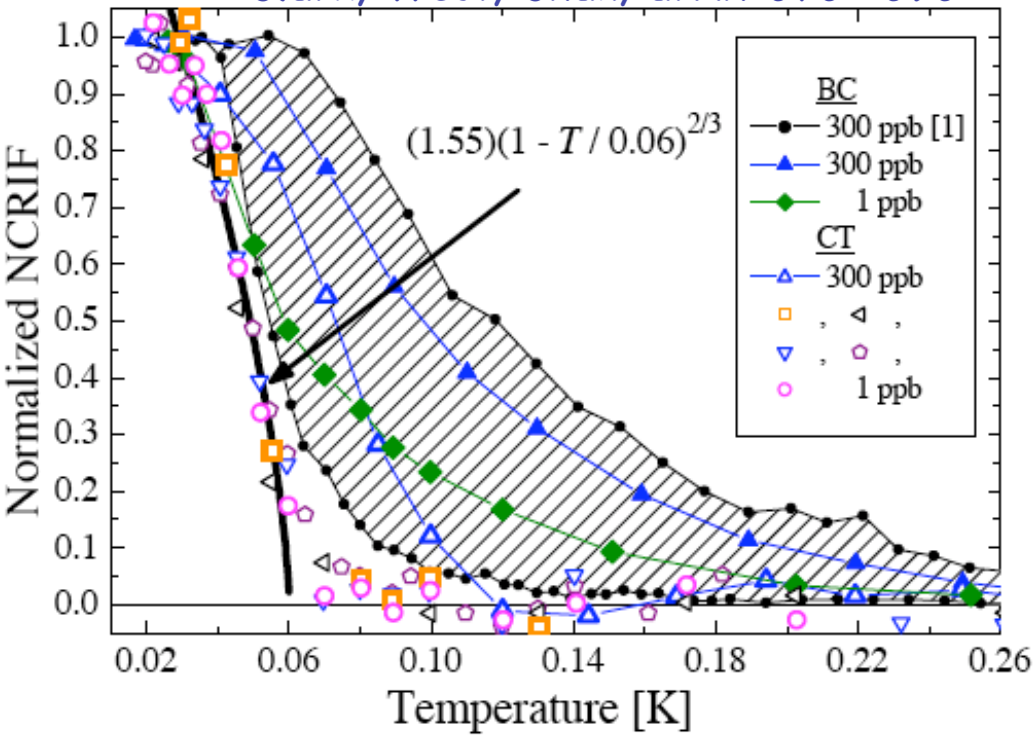

- Kim and Chan find an excess specific heat below 100 mK, a broad peak at ≈75 mK, present also for $x_{3He} \approx 10^{-9}$

Comments:

- no doubt that the NCRI is strongly dependent on some sort of defects (unlikely grain boundaries, perhaps dislocations)
- classical explanations (relaxation mechanism, glass) are incompatible with experiments
- overall picture is still confused

Some basic questions for Many-Body Theory

- Is the ground state of ^{4}He commensurate or is it incommensurate?

Commensurate: n^0 of atoms = n^0 of sites

Incommensurate: n^0 of atoms $\neq$ n^0 of sites

in other words: are ground state vacancies present? (interstitials seem less likely)

- Does a commensurate solid ^{4}He have ODLRO?
- Is ODLRO present only if some sort of disorder (vacancies, grain boundaries,...) exists either as equilibrium or as metastable states?

Only microscopic MB theories are able to answer such questions

Microscopic theories based on Monte Carlo simulations

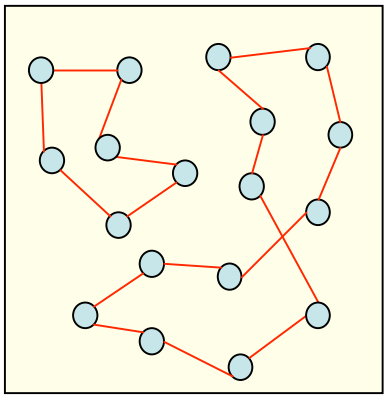

- Finite temperature:
  - Path Integral Monte Carlo (PIMC)
  - Worm Algorithm PIMC (add an open polymer in the picture)

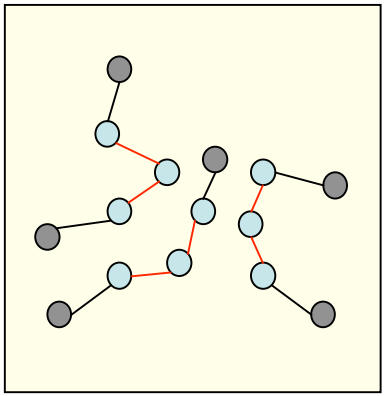

- Ground state:
  - Variational theory (Jastrow, Jastrow-Nosanow, Shadow wave function)
  - "exact" projection methods (Diffusion MC, Path Integral Ground State (PIGS), Shadow PIGS,...)

Present status:

points of agreement and points of disagreement

are present between the two approaches

Finite temperature (T≥0.1 K) PIMC results

(Ceperley and coll.; Prokof'ev and coll.)

- The commensurate state of solid ^{4}He (3D) is an "insulator": $n_0=0$, $\rho_s=0$
- Only in presence of extrinsic disorder (generic grain boundaries, walls, dislocations) one has supersolid behavior ($n_0\neq 0$, $\rho_s\neq 0$)
- Multiple vacancies form a bound state (Prokof'ev and coll.)

Interpretation of PIMC results (Prokof'ev and coll.)

- The ground state of solid ^{4}He is commensurate, no vacancies at low T

Ground state	Variational theory (SWF)	"Exact" T=0 K states (SPIGS)
Multiple vacancies	unbounded	unbounded
Commensurate or incommensurate?	incommensurate	incommensurate, ... but $\tau\rightarrow\infty$?
Commensurate state	$n_0\neq 0$	undecided yet ($n_0 \leq 2.5\times10^{-8}$)
Incommensurate state	$n_0\neq 0$	$n_0\neq 0$
Grain boundaries, walls	$n_0\neq 0$	$n_0\neq 0$

Solid ^{4}He: some important aspects

- Bragg scattering → translational broken symmetry (LRO)
- Very large Lindeman ratio at low density:

$$\frac{\sqrt{\left\langle \left| \vec{r}_i - \vec{R}_{eq} \right|^2 \right\rangle}}{a} \approx 0.26$$

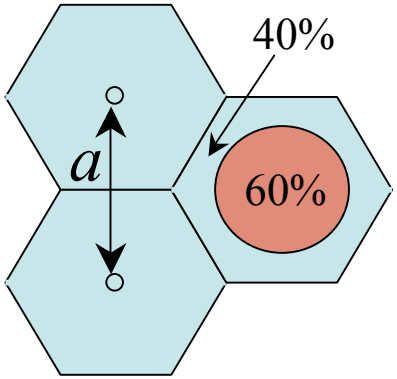

An atom has a 40% probability to be closer to the border of the Wigner Seitz cell than to the center of the cell

- Solid helium is a very soft solid
- One can grow almost perfect crystals (but it is not easy): large single crystal with very few dislocations

Vacancy-interstitial pairs (VIPs)

Evidence from theory

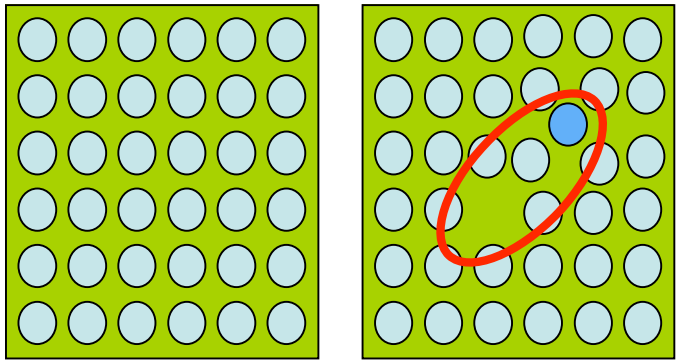

- Even in a commensurate state (n° lattice sites = n° atoms) one finds the presence of vacancy-interstitial pairs (VIPs)
- These VIPs are not excitations but simply fluctuations of the lattice; they are part of the large zero-point in the ground state of the solid
- The term "pairs" is used to underline the origin of these zero-point processes.
- Are VIPs unbound?

  Yes for SWF variational theory

  Not clear yet for exact ground state
- (SPIGS) VIP frequency: ≈1 every 10^3 MC steps with 180 ^{4}He atoms $\Rightarrow X_{vip} \approx 5.6 \times 10^{-6}$

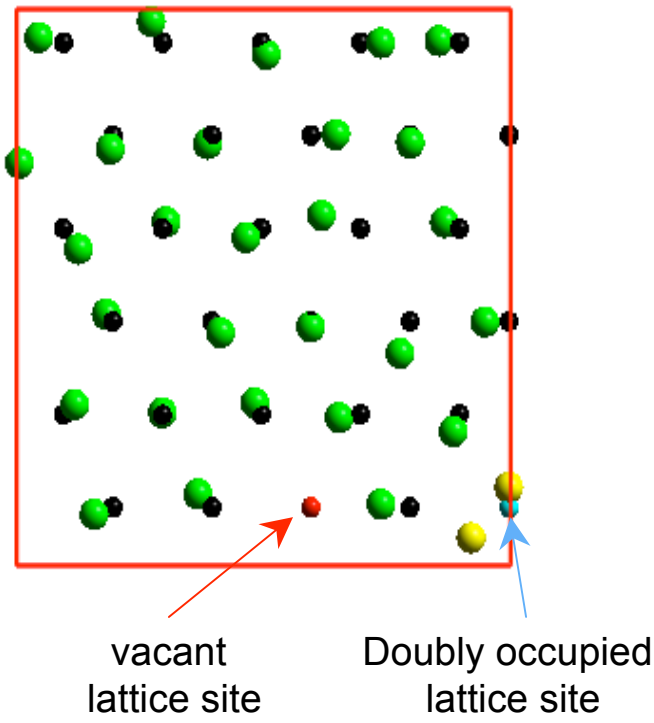

vacancy excitation spectrum (SWF result)

Galli, Reatto, Phys.Rev.Lett. 90, 2003;
Galli, Reatto, J.Low Temp.Phys. 134, 2004

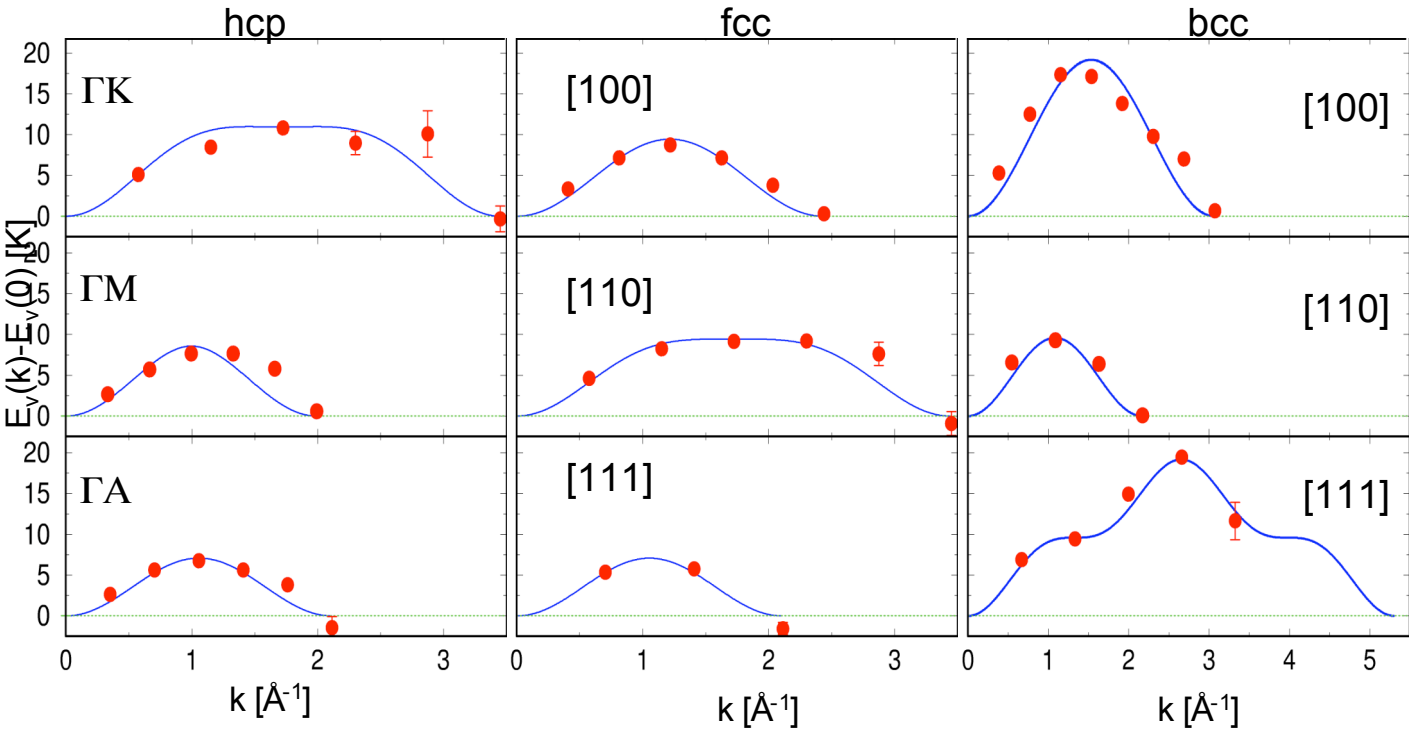

- SWF result
- n.n. jump model best fit

Near melting density

$\rho=0.029$ Å^{-3}

$m^*=0.31m_4$
$m^*=0.39m_4$ (ΓA)

$m^*=0.39m_4$

$m^*=0.3m_4$

residence time (hcp)

$$\tau = \frac{h}{\Delta} \cong 0.6 \times 10^{-11}\,\text{sec}$$

only 4 (and 2 in bcc) time larger than the period of high frequency phonon in the crystal

- Vacancy very mobile, in agreement with recent experiments

Andreeva et al., J.Low Temp.Phys. 110, 1998

- Band width decreases at larger density

The results are variational, exact results are not yet available

Projector QMC methods: Path Integral Ground State

Sarsa, Schmidt, Magro, J.Chem.Phys., 113, 2001

Path Integral representation of the propagator: $e^{-\tau\hat{H}} = \left(e^{-\frac{\tau}{P}\hat{H}}\right)^P$

$$\Psi_0(R) = \lim_{\tau\to\infty} \int dR_1 \cdots dR_P \left\langle R\left|e^{-\frac{\tau}{P}\hat{H}}\right|R_P\right\rangle \times \cdots \times \left\langle R_2\left|e^{-\frac{\tau}{P}\hat{H}}\right|R_1\right\rangle \Psi_T(R_1)$$

First approximation: finite imaginary time propagation

$$\Psi_0(R) \cong \int dR_1 \cdots dR_P \left\langle R\left|e^{-\frac{\tau}{P}\hat{H}}\right|R_P\right\rangle \times \cdots \times \left\langle R_2\left|e^{-\frac{\tau}{P}\hat{H}}\right|R_1\right\rangle \Psi_T(R_1)$$

Second approximation: the exact propagator is not known, short time approximation with $\delta\tau=\tau/P \ll 1$ (es. pair-product)

Path Integral Ground State (PIGS) wave function, Ψ_τ:

$$\Psi_\tau(R) = \int \left[\prod_{j=1}^{P} dR_j\, G(R_{j+1}, R_j, \tfrac{\tau}{P})\right] \Psi_T(R_1)$$

→ TEST of convergence in τ ($\tau\to\infty$) and accuracy of G ($\delta\tau\to 0$)

Projector QMC methods: Path Integral Ground State

Sarsa, Schmidt, Magro, J.Chem.Phys., 113, 2001

- Classical-Quantum mapping:

$$\frac{\langle \Psi_0 | \hat{O} | \Psi_0 \rangle}{\langle \Psi_0 | \Psi_0 \rangle} \cong \int \prod_{i=1}^{2P+1} dR_i \; \hat{O}(R_{P+1}) \frac{\Psi_T(R_1) \prod_{j=1}^{2P} G(R_j, R_{j+1}, \frac{\tau}{P}) \Psi_T(R_{2P+1})}{\langle \tilde{\Psi}_0 | \tilde{\Psi}_0 \rangle}$$

$$p(R_1, \cdots, R_{2P+1})$$

Ground state averages are equivalent to canonical averages of a classical system of special interacting linear polymers:

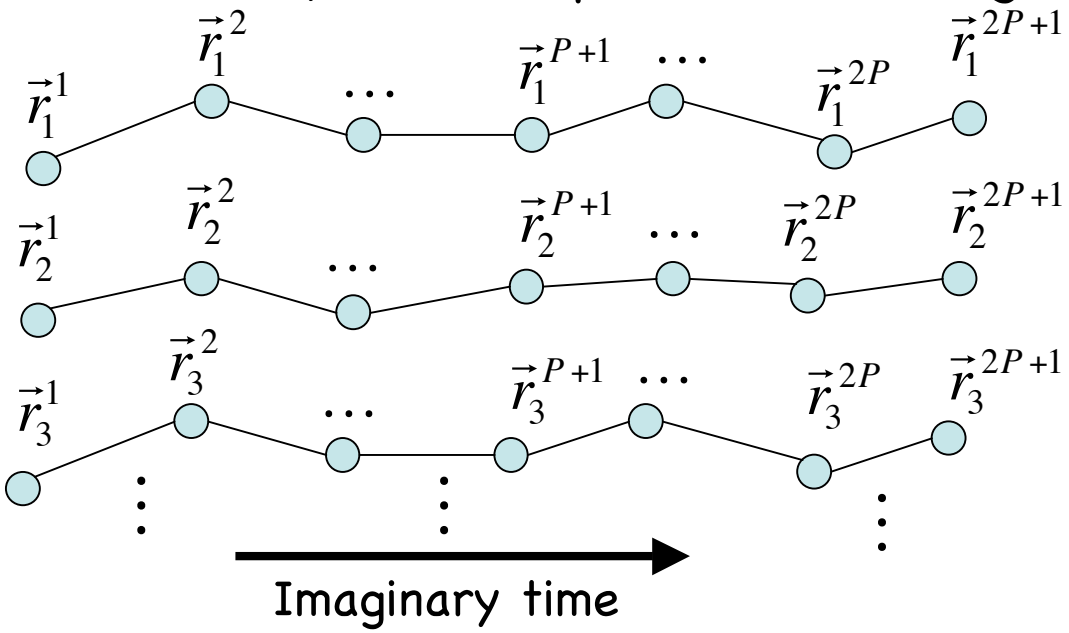

- P projections: linear polymers with 2P+1 atoms
- Monte Carlo sampling (Metropolis) of 3N·(2P+1) degree of freedom

$\vec{r}_{i=1,N}^{\,l=1,2P+1}$ ← imaginary time, ← particle

⇒ The whole imaginary-time evolution is sampled at each Monte Carlo step

Our "exact" tool: Projector QMC: from SWF to SPIGS

- SWF: single (variationally optimized) projection step of a Jastrow wave function

Vitiello, Runge, Kalos, Phys.Rev.Lett. 60, 1988

$$\Psi_T^{SWF}(R) = \int dS\, F(R,S)\, \Psi_T(S)$$

  - Implicit correlations (all orders)
  - Bose symmetry preserved

- SPIGS: "exact" T=0 projector method which starts from a SWF

Galli, Reatto, Mol. Phys. 101, 2003

$$\Psi_0(R) = \int dR_1..dR_P dS \left\langle R\left|e^{-\frac{\tau}{P}\hat{H}}\right|R_P\right\rangle \times \ldots$$

$$\cdots \times \left\langle R_2\left|e^{-\frac{\tau}{P}\hat{H}}\right|R_1\right\rangle F(R_1,S)\Psi_T(S)$$

  - Notice: unlike PIMC at finite T here no summation over permutation is necessary, this $\Psi_0(R)$ is Bose symmetric if Ψ_T is symmetric

Calculation of $\langle \Psi_0 | \hat{O} | \Psi_0 \rangle$

Classical analogy

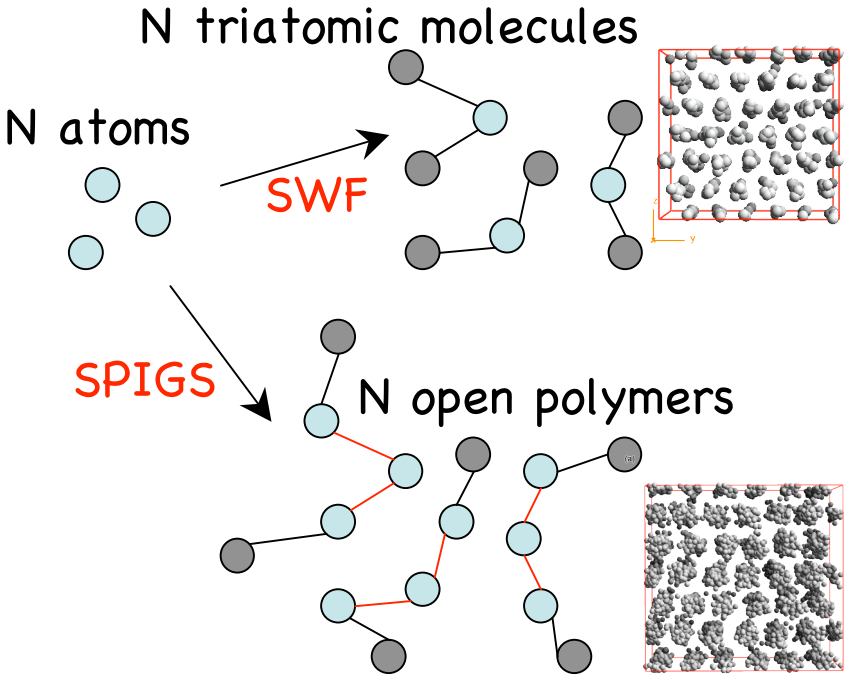

The whole imaginary time evolution is sampled at each MC step

Shadow variables

- Shadow variables are strongly correlated

Spontaneous translational broken symmetry for $\rho > \rho_o$

Crystalline order of ^{4}He atoms induced by many-body correlations introduced by the shadow variables

SWF simulation of hcp solid ^{4}He: projection of the coordinates of the real and shadow particles in a basal plane for 100 MC steps

- Shadow positions
- ^{4}He atom positions

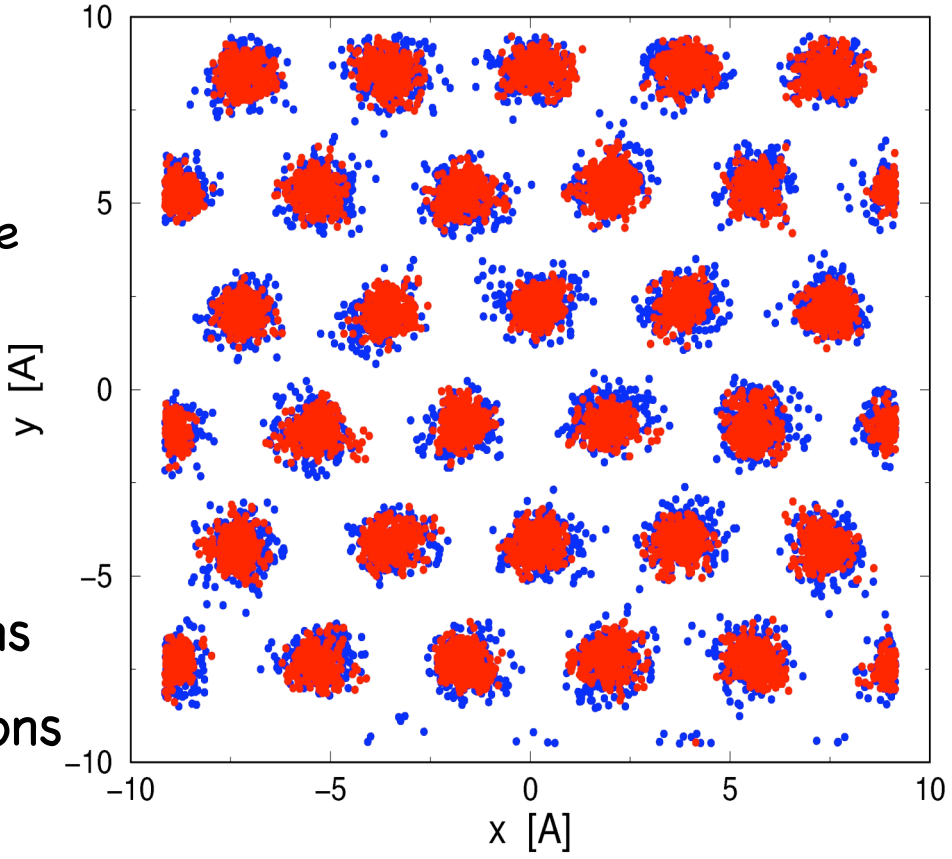

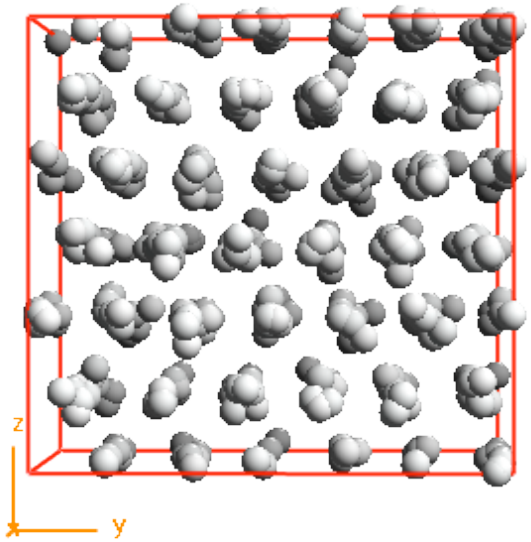

Lindeman ratio

SWF: 0.242(2)

Exp.: 0.263(6)

Presently SWF represents the best variational wave function of solid ^{4}He

Why a trial SWF ?

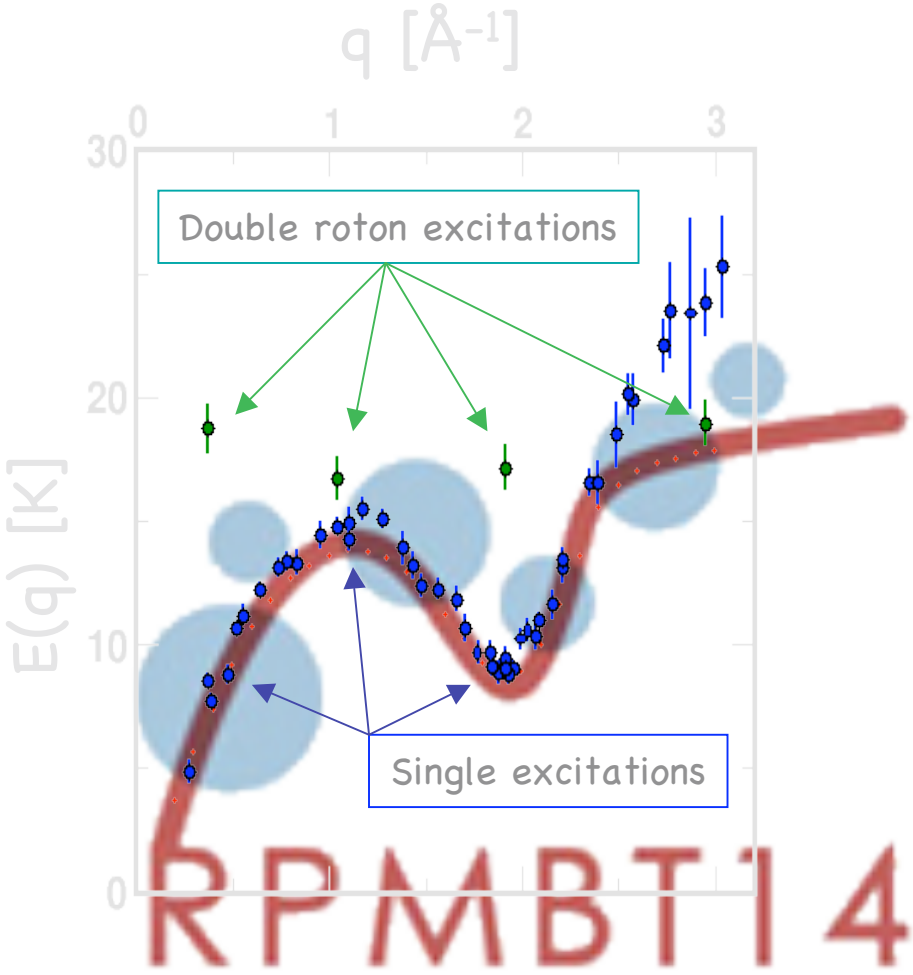

Excitations in the liquid phase turns out to be in good agreement with the logo

(Galli, Cecchetti, Reatto, PRL 1996;
Moroni, Galli, Fantoni, Reatto, PRB 1998)

good agreement also in the solid phase (longitudinal and transverse phonons)

(Galli, Reatto, PRL 2003;
Galli, Reatto, JLTP 2004;
Mazzi, Galli Reatto, AIP proceedings LT24, 2006)

SPIGS (Galli, Reatto, Mol. Phys. 101, 2003)

In principle the method is exact,

two parameters control convergence:

- $\tau/P \rightarrow$ accuracy of the short time propagator
- $P \rightarrow$ number of time slices

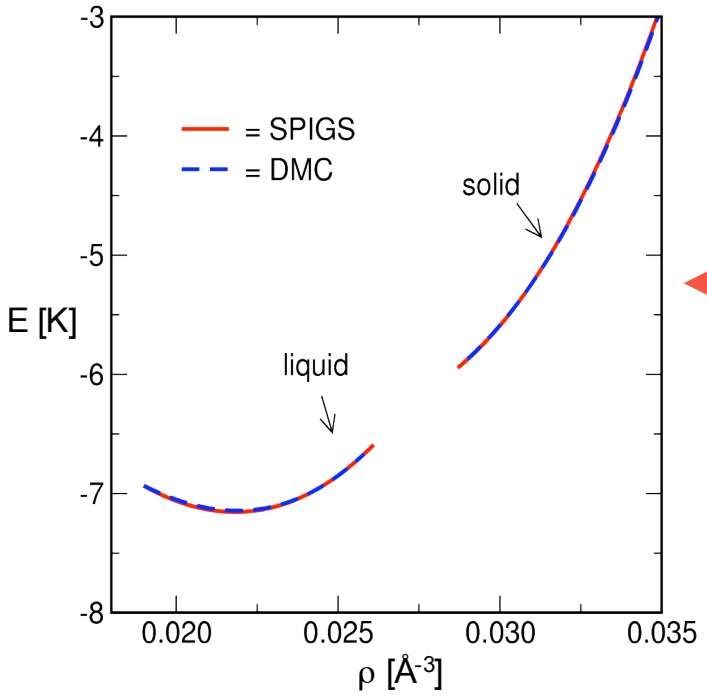

Example

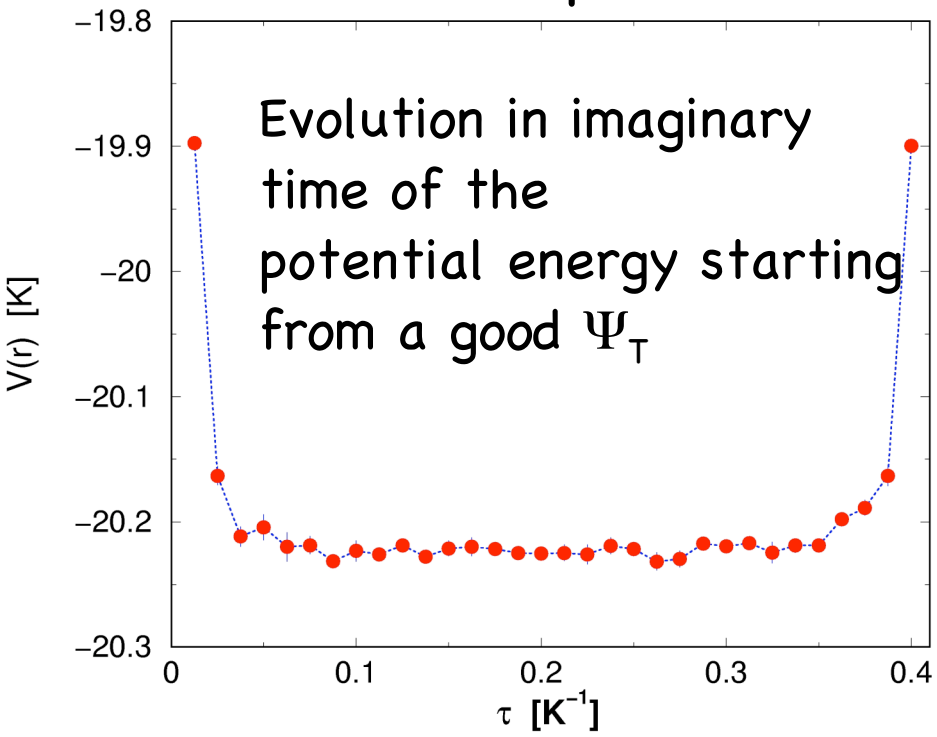

Equation of state of bulk ^{4}He (Aziz potential, 1979):

comparison between the SPIGS and the DMC methods

SPIGS: the solid phase

(Galli, Reatto, Mol. Phys. 101, 2003)

- Solid phase: spontaneously broken translational symmetry
- Lindemann ratio $\sqrt{|r-R|^2}/a = 0.257(4)$

  Exper. 0.263(6) (Burns, Isaacs PRB 55, '97)

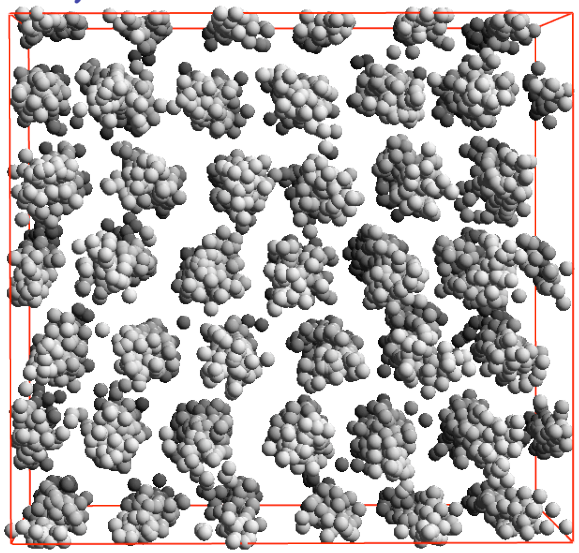

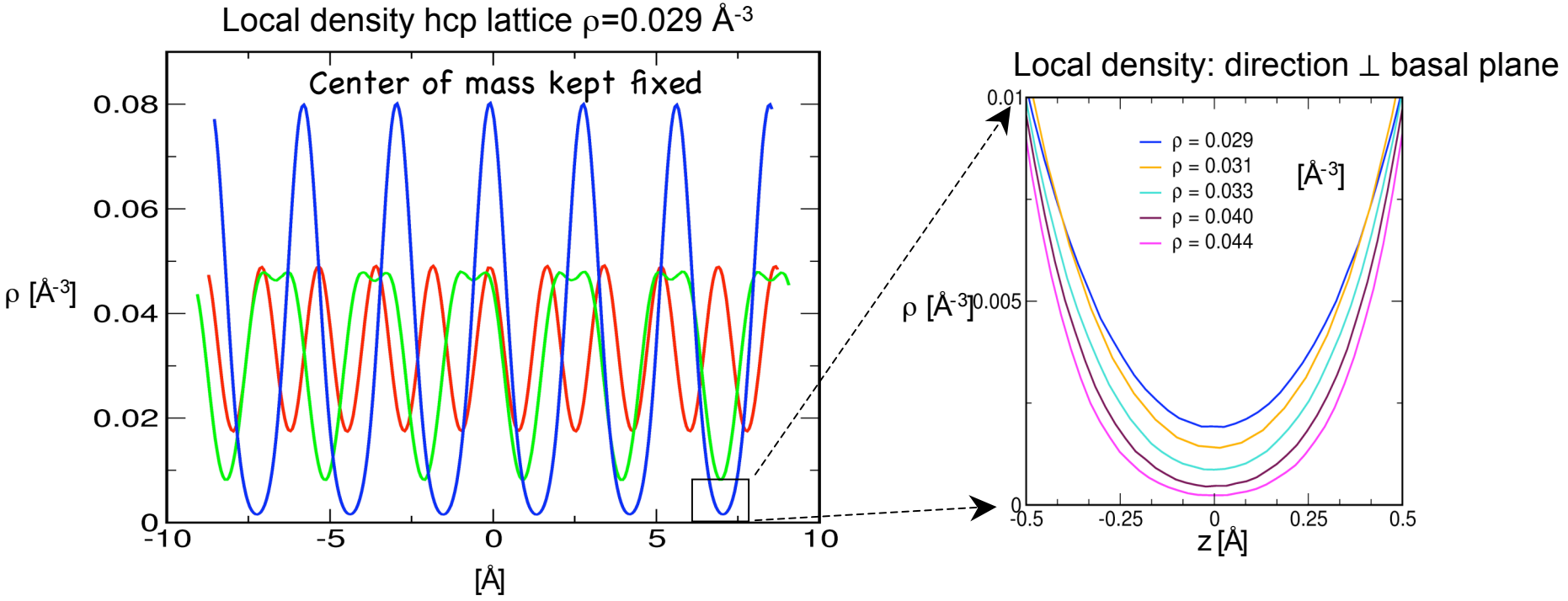

Variational theory of a quantum solid

In the framework of variational theory of quantum solids the wave functions fall in two categories:

1. Ψ has explicit translational broken symmetry, for instance by localizing the atoms around the assumed lattice sites $\{\vec{R}_i\}$

$$\Psi(\vec{r}_1,..,\vec{r}_N) = \Psi_J \times \prod_i^N e^{-C\left|\vec{r}_i - \vec{R}_i\right|^2}$$

(Jastrow+Nosanow)

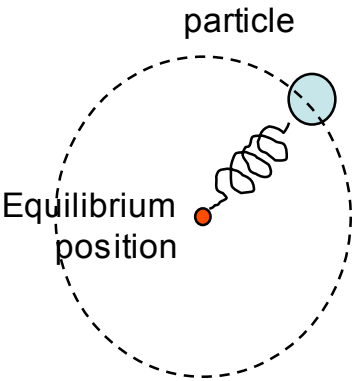

→ Sum over permutation to get Bose Symmetry

by construction this wave function describes a commensurate solid

2. translational invariant Ψ, first example:

$$\Psi_J(\vec{r}_1,..,\vec{r}_N) = \prod_{i<j}^N f\left(\left|\vec{r}_i - \vec{r}_j\right|\right)$$ (Jastrow)

Second example: Shadow Wave Function

SPIGS versus PIGS (2D)

- Imaginary time evolution from different trial wave function:
  expectation value of the energy

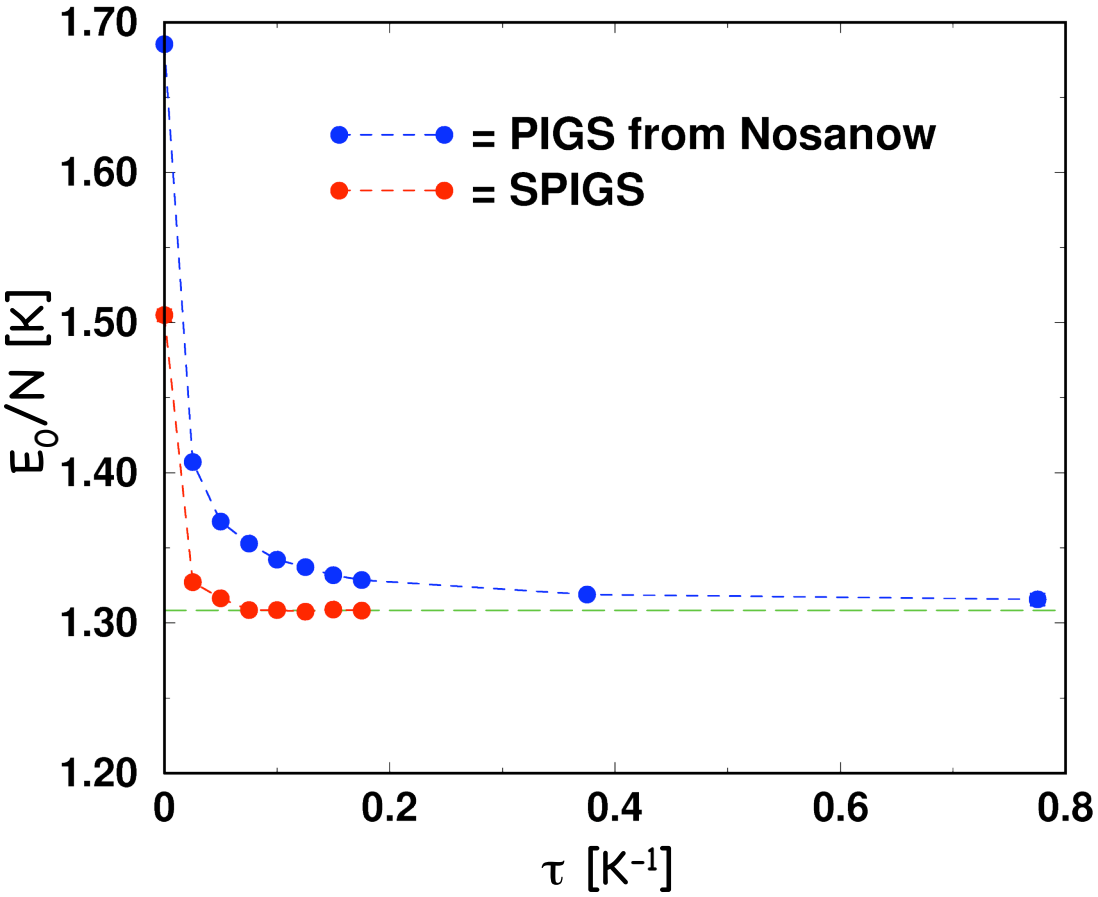

- PIGS reaches convergence only for $\tau > 0.8$ K^{-1}

2D solid ^{4}He ρ=0.765 Å^{-2}, triangular lattice

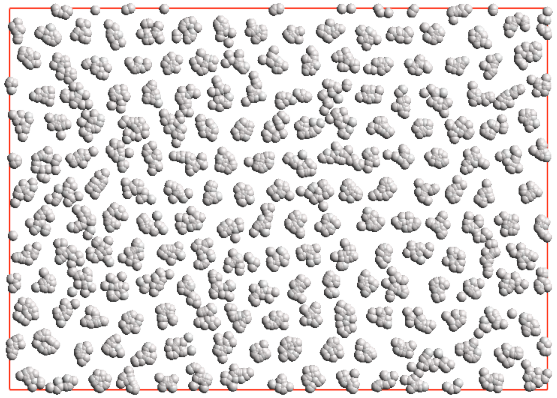

GFMC: Whitlock et al., PRB 38, '88

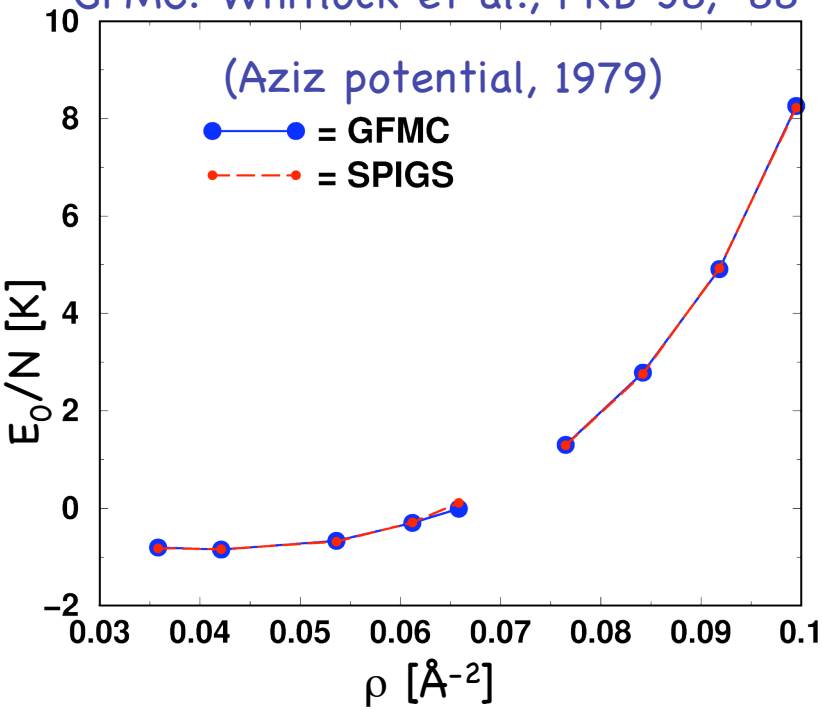

Off Diagonal Long Range Order

- The one-body density matrix:

$$\rho_1(\vec{r},\vec{r}') = \left\langle 0\left|\hat{\Psi}^+(r)\hat{\Psi}(r')\right|0\right\rangle = N\int dr_2\cdots dr_N \Psi_0^*(r,r_2,\cdots,r_N)\Psi_0(r',r_2,\cdots,r_N)$$

- Momentum distribution:

$$n(\vec{k}) = V^{-1}\int d\vec{r}\, d\vec{r}'\, \rho_1(\vec{r},\vec{r}')e^{i\vec{k}\cdot(\vec{r}-\vec{r}')}$$

- BEC $\Leftrightarrow$ ODLRO

$$\lim_{|\vec{r}-\vec{r}'|\to\infty} \rho_1(\vec{r},\vec{r}') = \rho n_0$$

$$n(\vec{k}) = (2\pi)^3 \rho n_0 \delta(\vec{k}) + n'(\vec{k})$$

- Presence of ODLRO allows to define a local phase → NCRI

QMC simulations
In the liquid

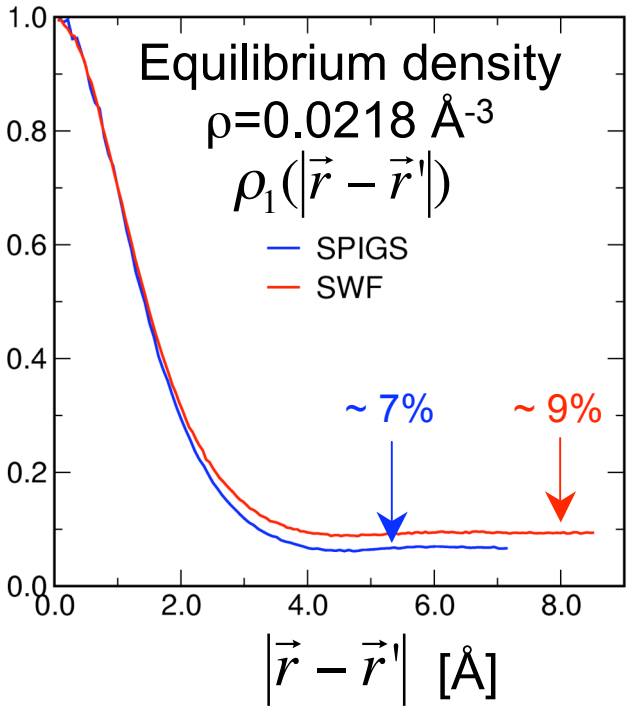

QMC: calculation of the one-body density matrix

$$\rho_1(\vec{r},\vec{r}') = N\int dr_2\cdots dr_N \Psi_0^*(\vec{r},\vec{r}_2,\cdots,\vec{r}_N)\Psi_0(\vec{r}',\vec{r}_2,\cdots,\vec{r}_N)$$

- One of the open polymers is cut and the histogram of the relative distance of the two cut ends is computed
- We have studied commensurate and incommensurate solid ^{4}He with SPIGS: the periodic boundary conditions forces the structure of the solid.
- No "mixed", only pure estimator (exact ground state ρ_1 if τ is large enough!)

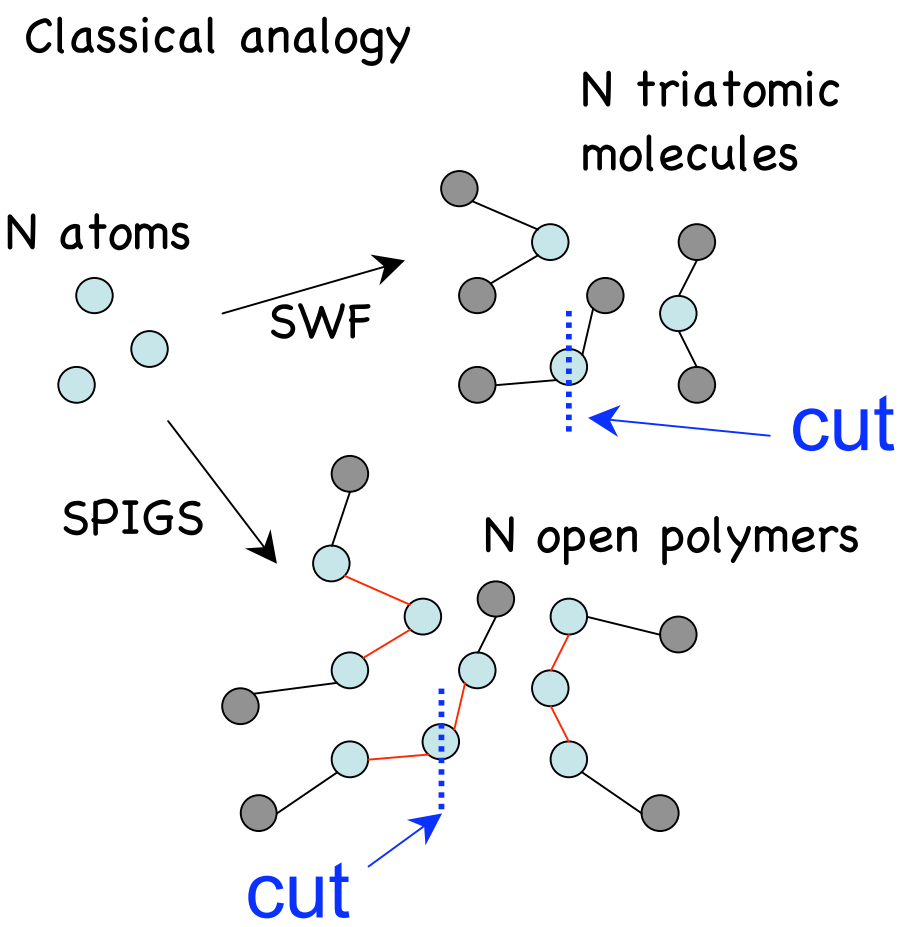

ODLRO - Commensurate state

SWF results: ODLRO in commensurate solid ^{4}He

Galli, Rossi, Reatto, Phys.Rev. B 71, 2005

- ODLRO is present: $n_0 \approx 5 \pm 2 \times 10^{-6}$ at melting and for a finite range of densities (up to 54 bars)
- No finite-size effects
- Key process is the presence of VIPs

ODLRO: microscopic origin

$$\rho_1(\vec{r},\vec{r}') = \left\langle 0 \left| \hat{\Psi}^+(\vec{r}) \hat{\Psi}(\vec{r}') \right| 0 \right\rangle$$

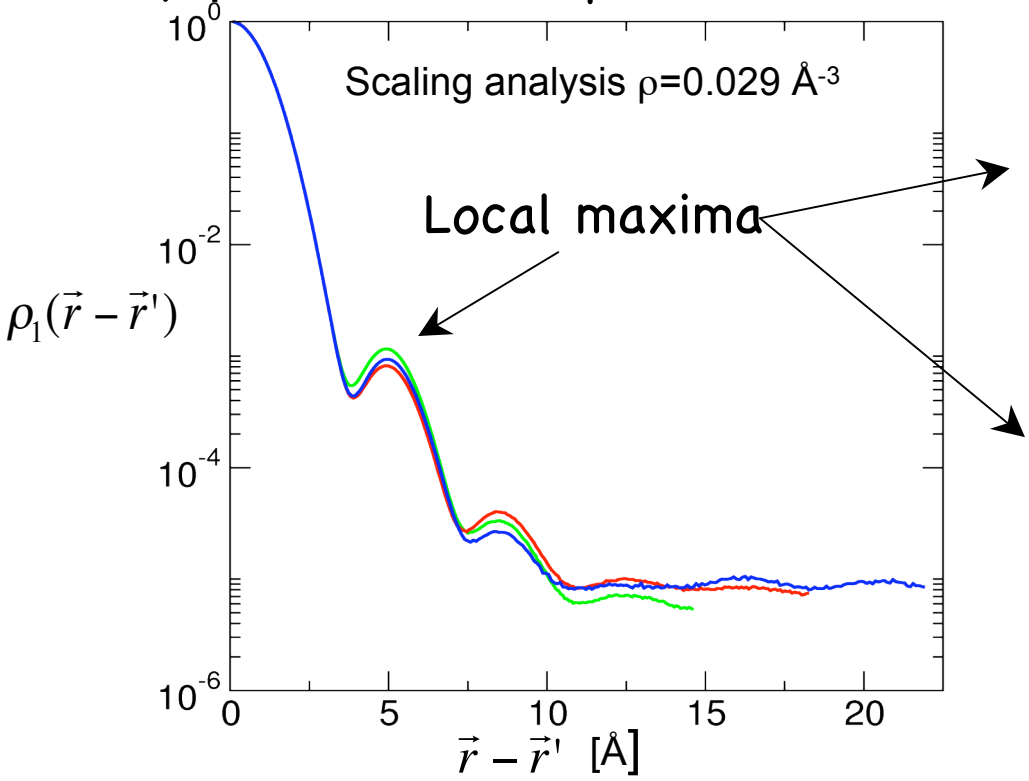

Snapshot of SWF trimers in a basal plane

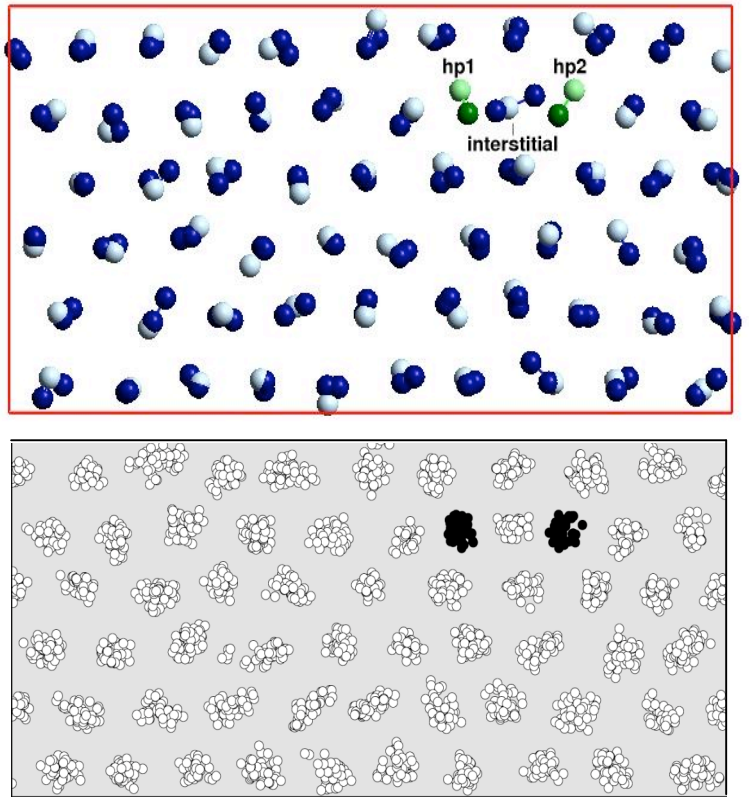

(S)PIGS: Permutation sampling

- projection procedure preserves the Bose symmetry if Ψ_T is Bose symmetric

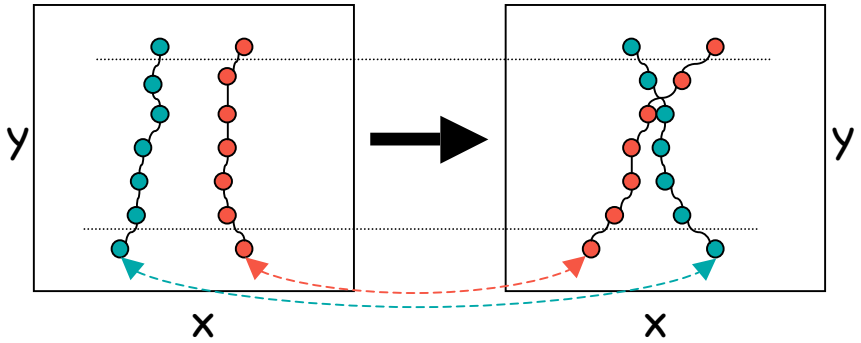

- No topological sampling problems
- It is important for off-diagonal properties in the solid phase
- Sampling scheme: Boninsegni JLTP (2005)
- also "swap" moves allowed in off-diagonal calculations

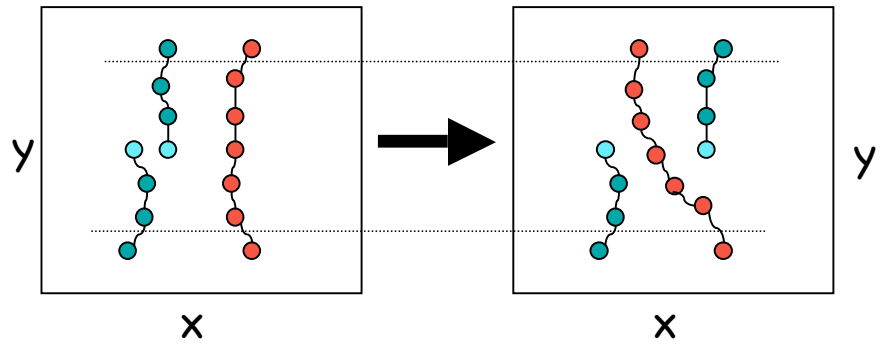

Off-diagonal calculation:

frequency of an accepted permutation cycle with N polymers

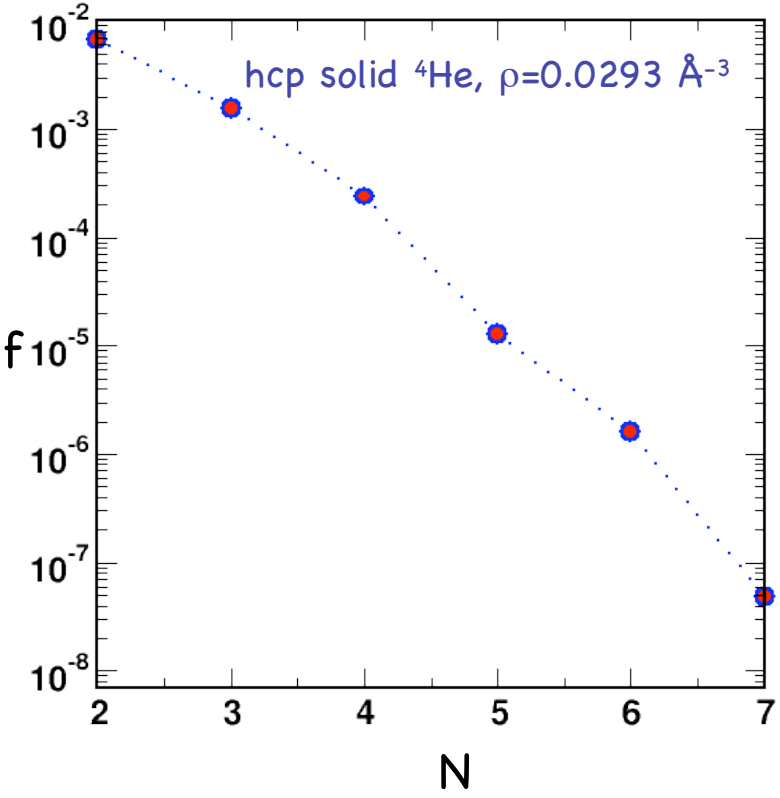

Frequency of an accepted permutation cycle is only about 5 times lower than in the liquid phase

ODLRO - Commensurate state

One-body density matrix: SPIGS results

- Calculations of the one-body density matrix in hcp solid ^{4}He at melting density ρ=0.0293 Å^{-3} with SPIGS
- Pair-product approximation: $\delta\tau$=(40 K)$^{-1}$
- Sampling along nearest neighbour direction
- Plateau dramatically reduced by the projection procedure
- Presently we can give only an upper bound: n_0<2.5x10^{-8}
- Calculation with larger τ are under way
- What is missing in SWF?

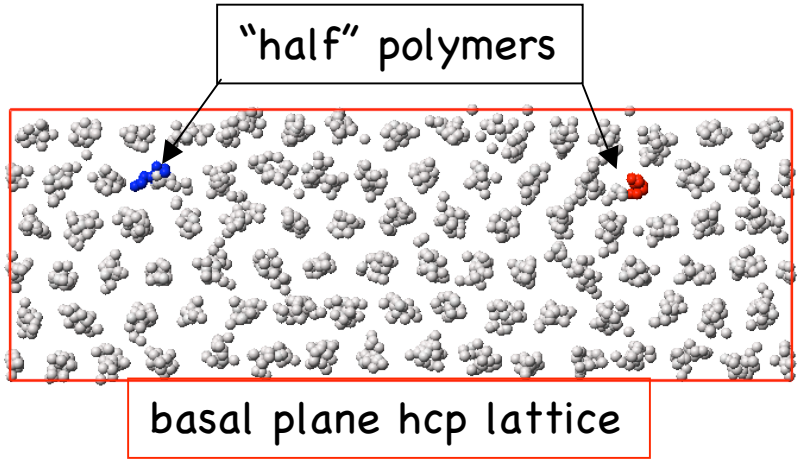

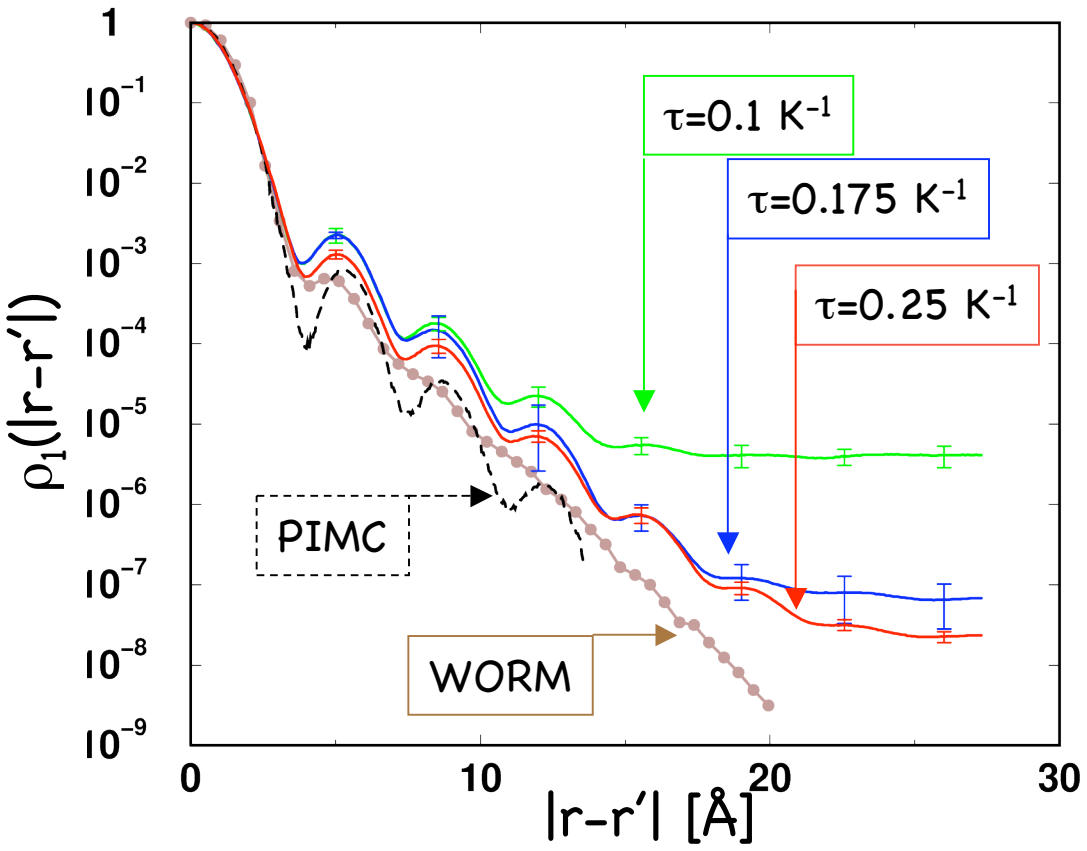

ODLRO - Commensurate state

One-body density matrix in 2D: SPIGS results

- Calculations of the one-body density matrix in 2D solid ^{4}He above meltin density ρ=0.765 Å^{-2} with SPIGS
- Sampling along nearest neighbour direction
- Pair-product approximation: $\delta\tau$=(40 K)$^{-1}$
- Plateau dramatically reduced by the projection procedure
- Convergence to exponential decaying tail in agreement with result from PIGS with Nosanow wave function

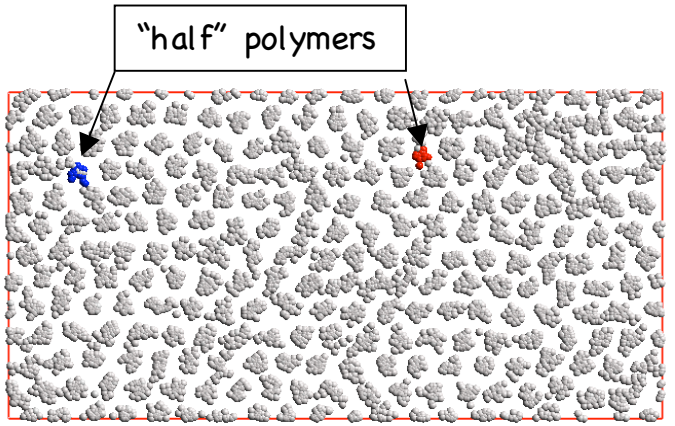

2D solid ^{4}He ρ=0.765 Å^{-2}, triangular lattice

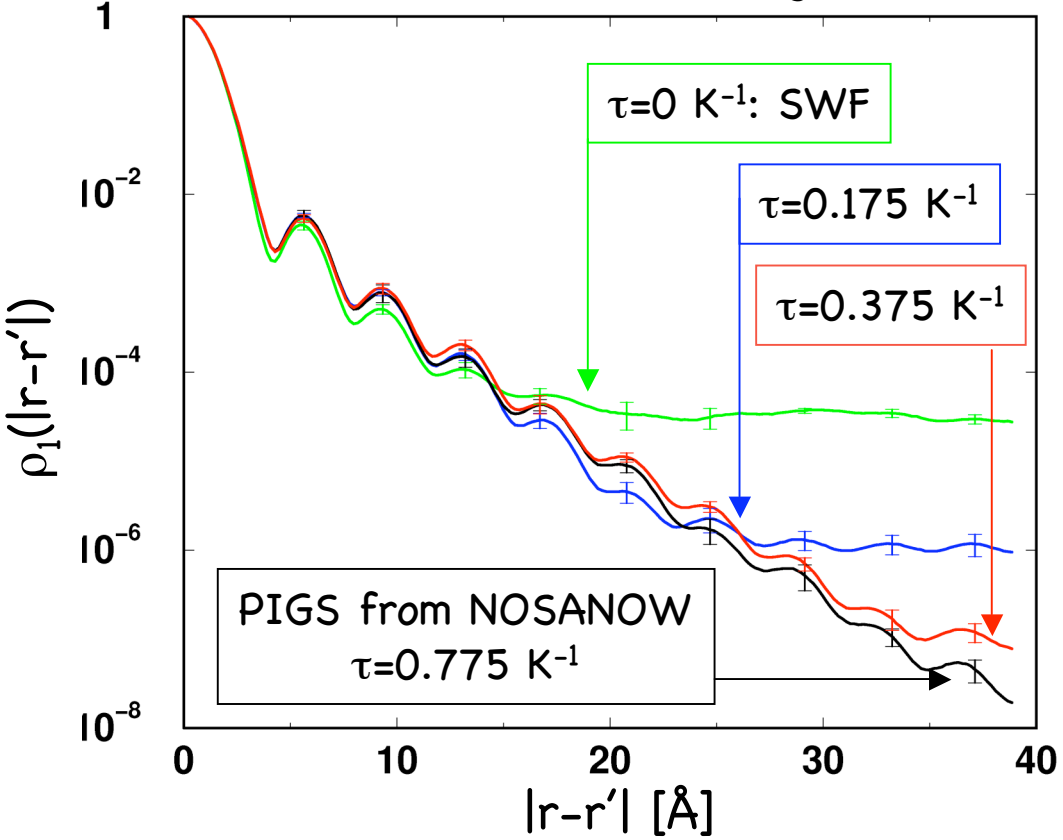

Incommensurate solid, SPIGS results: ODLRO in solid ^{4}He with vacancies

(Galli, Reatto, PRL 2006)

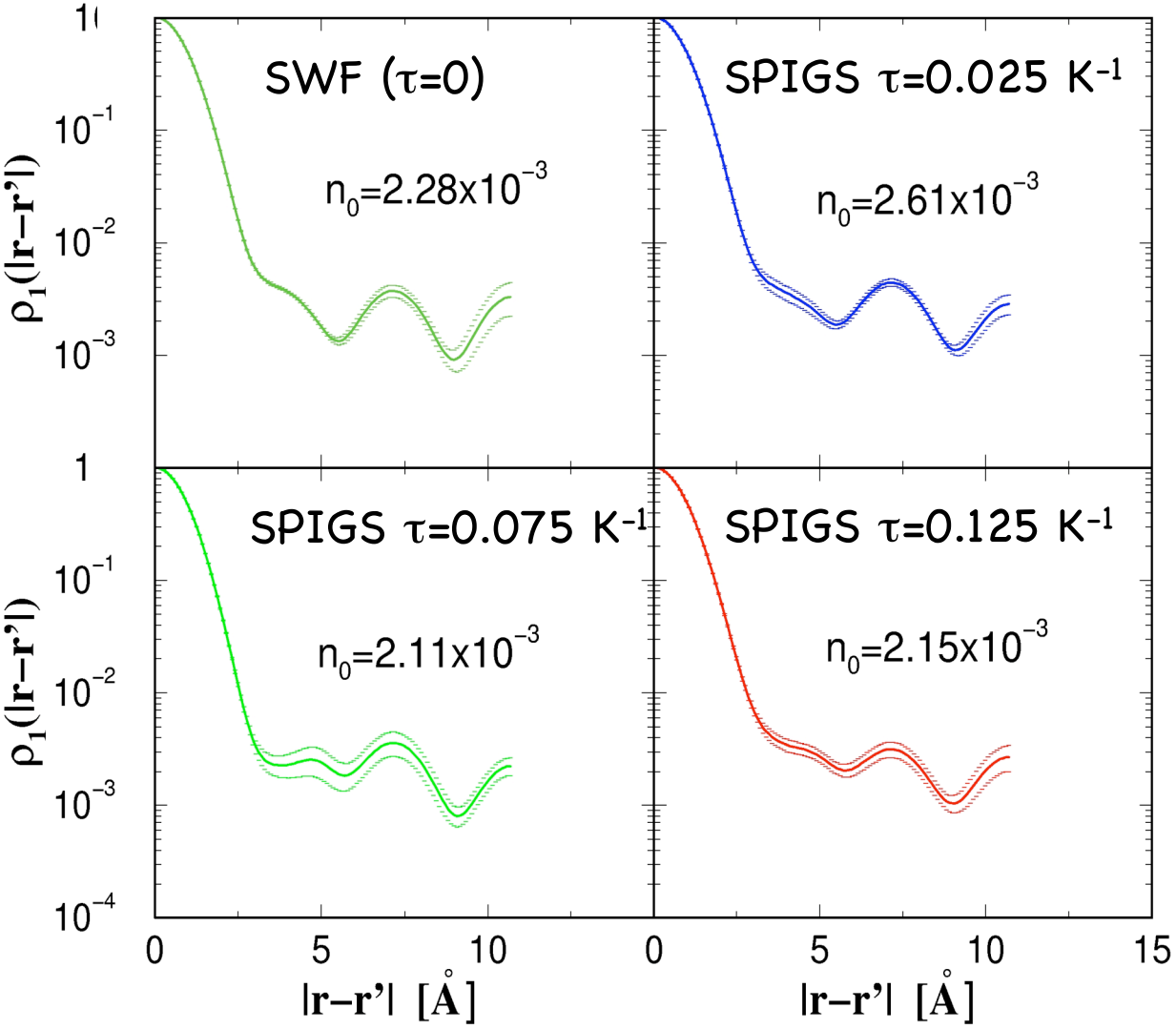

- 1 vacancy and 107 atoms
- Sampling along nearest neighbors direction
- fcc ρ=0.031 Å^{-3} P=54 bars pair-product approximation $\delta\tau$=(40 K)$^{-1}$
- ODLRO is still present with SPIGS

ODLRO - Incommensurate state

Latest results of ODLRO in hcp ^{4}He with vacancies at melting density

Fixed vacancy concentration:
X_v=1/287
ρ=0.0293 Å^{-3}

BEC fraction:
$n_0 \approx 5 \times 10^{-4}$
BEC fraction per vacancy:
$n_0^{(v)} = 0.144$

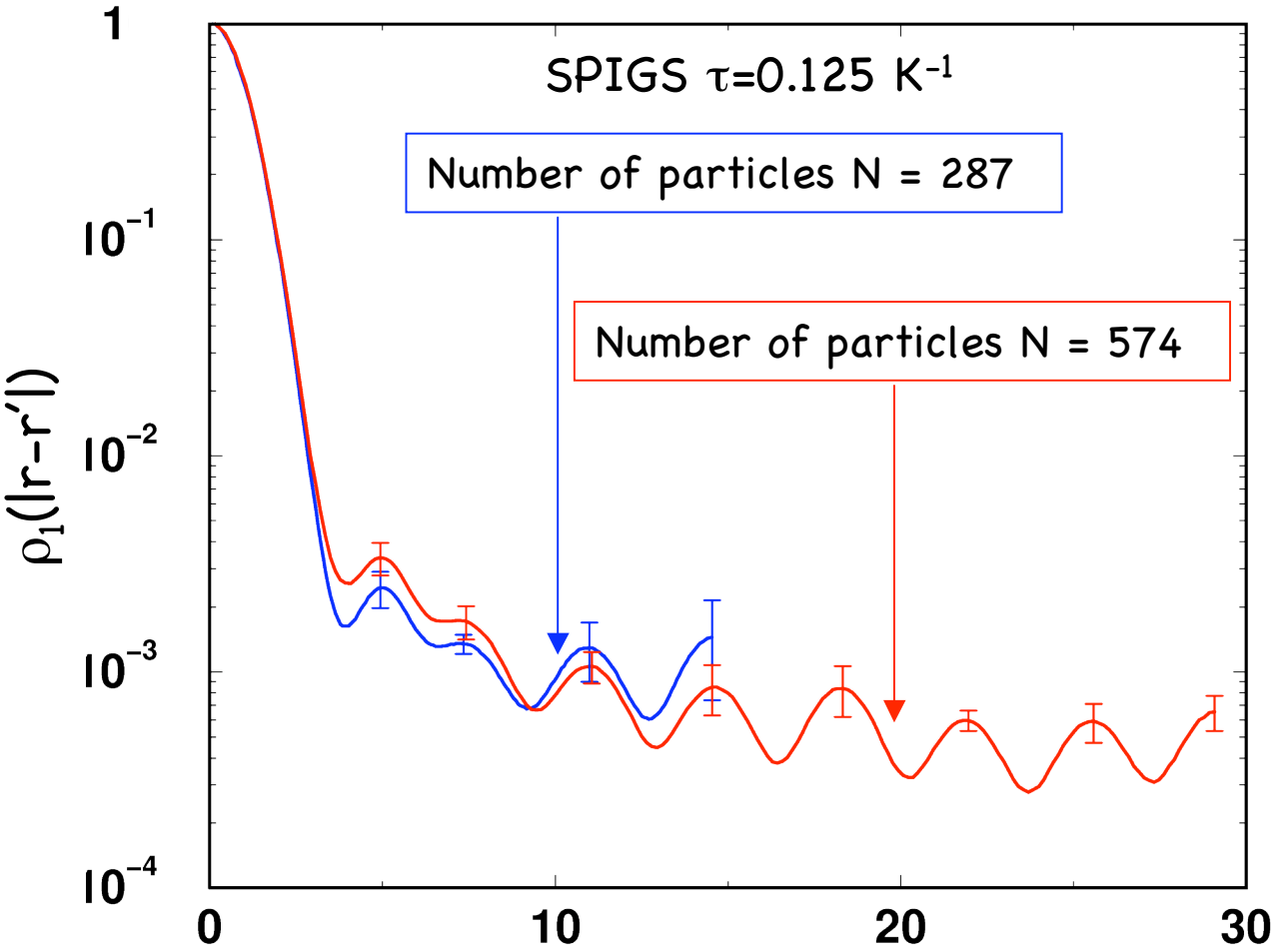

No remarkable effect on n_0 by enlarging the system with fixed X_v

Multiple vacancies: unbound state or phase separation?

It has been stated that 3 vacancies form a tight bound state (Boninsegni et al., PRL 2006) and multiple vacancies give phase separation

Our results: study of 1,2 and 3 vacancies at fixed concentration of vacancies X_v=1/179

Computation for hcp at ρ=0.0293Å^{-3}

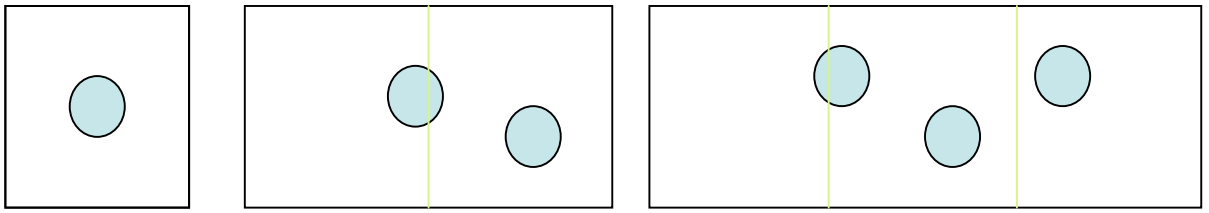

Vacancy activation energy: 16.4±0.8 K, 31.5±1.5 K, 2 x (15.75±0.75) 43.0±2.0 K 3 x (14.33±0.67)

- Vacancy activation energies seem compatible with a small attractive interaction (0.3-0.7 K) between vacancies

Multiple vacancies: unbound state or phase separation?

Computation for hcp at ρ=0.0293Å^{-3}

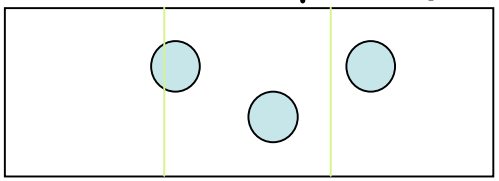

τ=0.25 K^{-1}

Notice for simulators: very long MC runs are needed

- vacancy-vacancy correlation function $g_{vv}(r)$ for a system of 3 vacancies

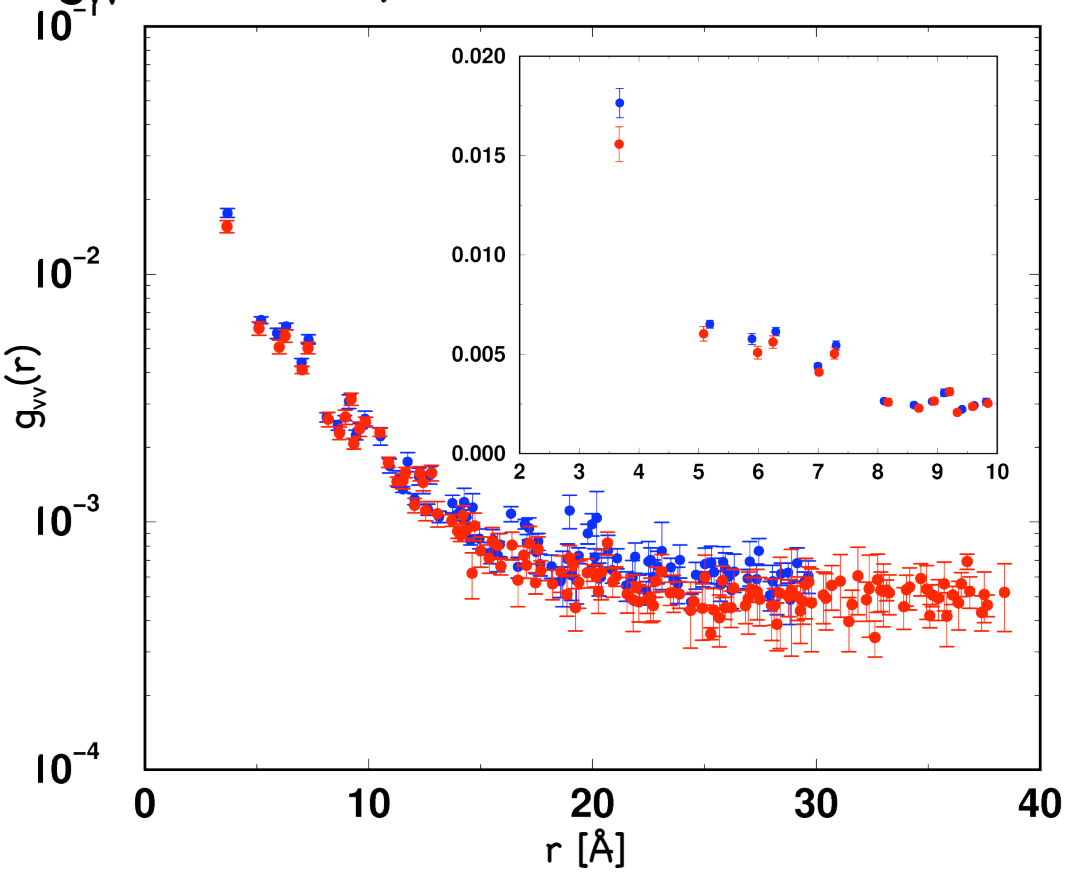

Probability P to find vacancies at distance < r

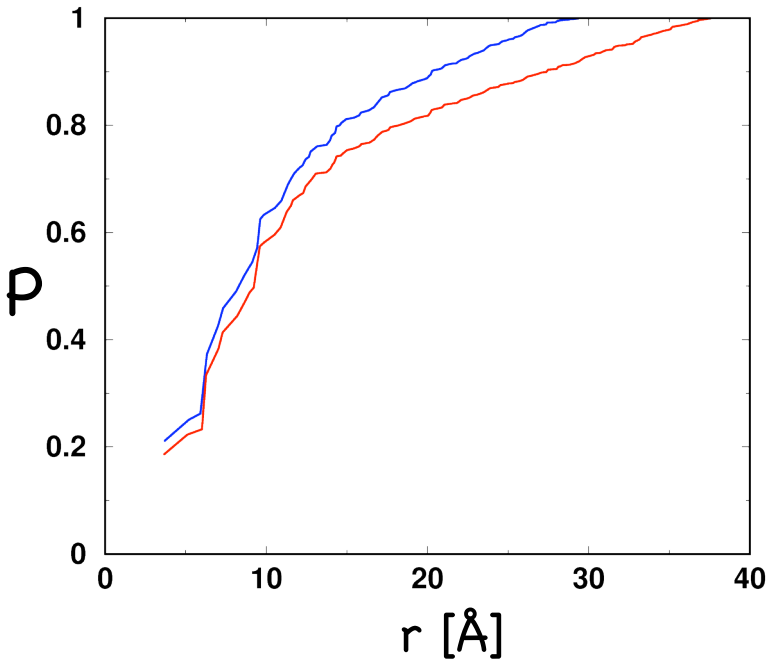

- g_{vv}: plateau at large distances
- g_{vv}: depression at small distance when system gets larger

Conclusion:

2 and 3 vacancies do not form a bound state

SPIGS: Vacancy-vacancy interaction

- Recently we have started a systematic study of the interaction between vacancies also in presence of ^{3}He impurities:

ρ=0.031 Å^{-3} Commensurate crystal N=180	Δe_{1v} [K]	Δe_{2v} [K]	Δe_{3v} [K]	Δe_{4v} [K]	Δe_{5v} [K]
pure ^{4}He	21.3±0.4	40.6±0.6 (-2.0)	56.9±0.6 (-7.0)	73.0±0.4 (-12.2)	89.3±0.5 (-17.2)
^{4}He + 1 ^{3}He	21.4±0.4	41.6±0.2 (-1.2)	58.9±0.4 (-5.3)	73.6±0.4 (-12.0)	87.1±0.5 (-19.9)

- Attractive interaction is again evident
- No particular effect of ^{3}He on the interaction between vacancies
- The vacancy moves freely: no evidence of bound state with ^{3}He atoms

Is the ground state of bulk solid ^{4}He commensurate or incommensurate?

- Early theoretical works were based on the assumption of zero-point vacancies (Andreev and Lifshitz, JETP 93 1969; Chester, Phys.Rev.A 2 1970)
- If ground state vacancies are present this will have significant effects on low T behavior of solid ^{4}He (phenomenological theory by P.W. Anderson, et al. Science 310 2005)
- Naive answer: it is commensurate because computation of $\langle \Psi_0 | \hat{H} | \Psi_0 \rangle$ for the perfect solid with one vacancy allowed to estimate a vacancy formation energy $\Delta e_v > 0$
- This argument is not conclusive: one has deduced Δe_v from computation of the ground state energy of two different systems, Δe_v is a derived quantity as an estimate of the extra energy due to the presence of one additional vacancy

Example of computation of Δe_v

- System 1: commensurate state

  108 atoms in a cubic box of volume V with periodic boundary conditions in which fcc lattice fits exactly

Local density $\rho(\vec{r})$ has 108 maxima

$\Rightarrow$ n° sities = n° atoms

108 108

- System 2: incommensurate state

  107 atoms in the same box

Local density $\rho(\vec{r})$ has 108 maxima

$\Rightarrow$ n° sities $\neq$ n° atoms

108 107

Evolution in imaginary time τ starting from a fully optimized SWF

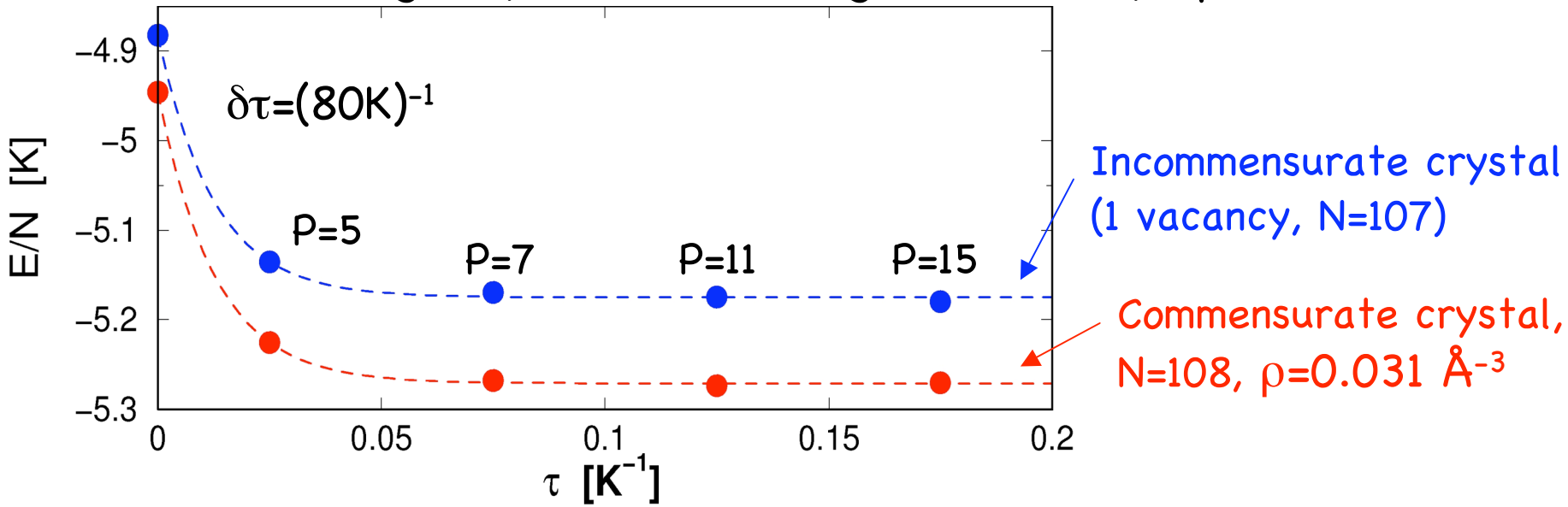

Both wave functions are non negative and represent two ground states: depending on N and box shape the ground state for this small system with pbc is commensurate or incommensurate

Commensurate or incommensurate?

Commensuration effects in small system makes difficult to answer this question, one has to analyze an extended system of $\mathcal{N}$ particles in a volume V so large that boundary conditions have a negligible role

⇒ Similar to what one has to do to treat vacancies in a classical system (Swope, Andersen, PRB 46, '92)

Consider translational invariant wave functions

I Example: Jastrow wave function $\Psi_J(\vec{r}_1,..,\vec{r}_{\mathcal{N}}) = \prod_{i<j}^{\mathcal{N}} e^{-\frac{1}{2}u(r_{ij})} / Q_{\mathcal{N}}^{1/2}$

(old argument by Chester)

Normalization constant: $Q_{\mathcal{N}} = \int d\vec{r}_1..d\vec{r}_{\mathcal{N}} \prod_{i<j}^{\mathcal{N}} e^{-u(r_{ij})}$

Ground state averages with $|\Psi_J|^2$ → N classical particles at $\beta^*=1/kT^*$ and with pair potential $v^*(r)$ such that $\beta^* v^*(r)=u(r)$

Normalization constant $Q_{\mathcal{N}}$ → canonical configurational partition function of this classical system

From analysis of $Q_{\mathcal{N}}$ of a classical solid → the lowest free energy corresponds to a state with a finite concentration $\overline{X}_v = (\mathcal{M} - \mathcal{N})/\mathcal{N}$ of vacancies

Consequence for the quantum system: Ψ_J of an extended system has a finite concentration of vacancies

$\mathcal{M}$: n° lattice sites
$\mathcal{N}$: n° particles

- Schematic landscape of probability distribution at high density (similarity with probability in configuration space of suitable classical particles)
- For a Jastrow wave function the overwhelming contribution to normalization $Q_{\mathcal{N}}$ comes from pockets with vacancies (finite concentration!)
- Conclusion: Ψ_J has a finite BEC (Reatto, Phys.Rev. 183, 1969) and a finite concentration of vacancies

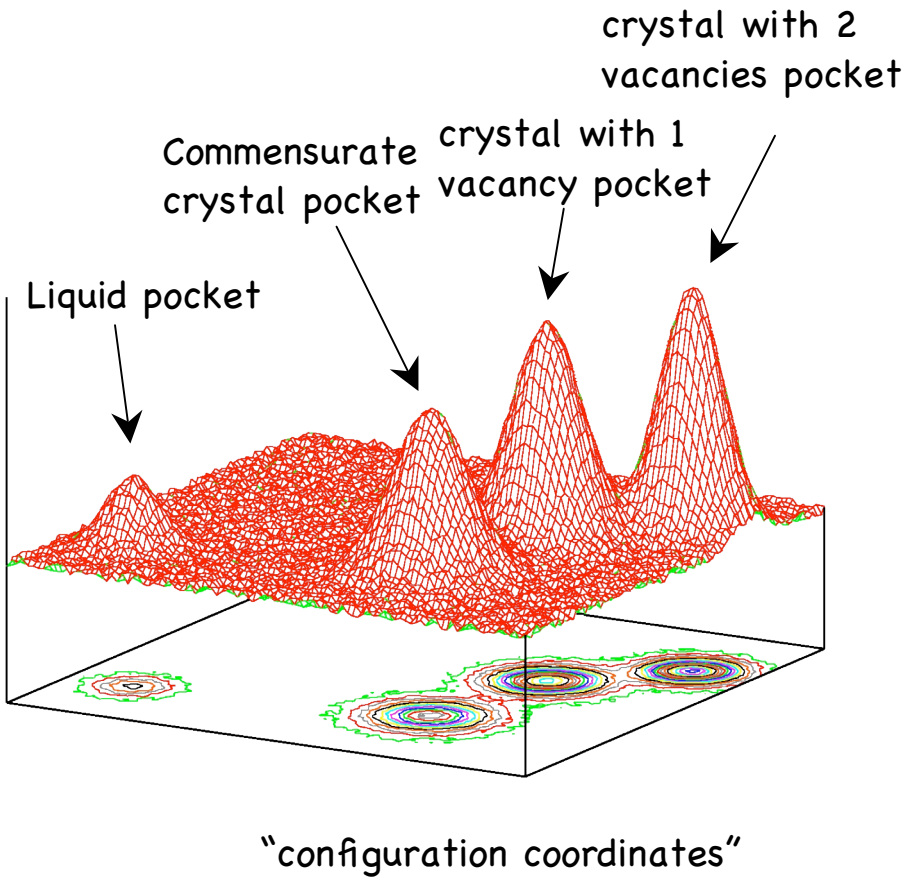

- Hodgdon and Stillinger (1995) have estimated this vacancy concentration; we have computed X_v with an accurate quantitative method:

  vacancy concentration $\overline{X}_v \approx (1.4 \pm 0.1)\ 10^{-6}$

- Standard MC computation for a small system: implicit normalization of Ψ_0 only in a single pocket, computed energy is biased by the choice of N and cell geometry (Q_N in a Monte Carlo computation is never computed)
- Ψ_J is unrealistic for solid ^{4}He, so this $\overline{X}_v$ is not very significant

Commensurate or incommensurate?

II Example: Shadow wave function $\Psi(R) = \phi_r(R) \times \int dS\, K(R,S) \times \phi_s(S) / Q_{\mathcal{N}}^{\frac{1}{2}}$

$$Q_{\mathcal{N}} = \int dR\, dS\, dS'\, \phi_r^2(R) K(R,S) K(R,S') \phi_s(S) \phi_s(S')$$

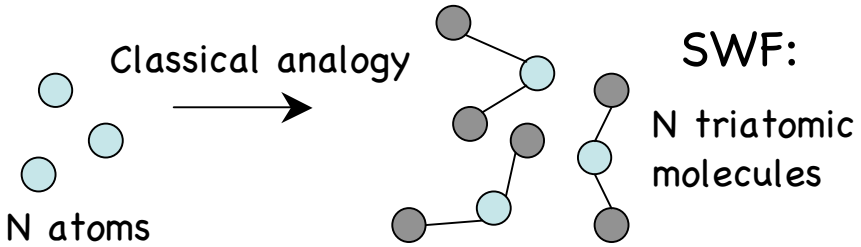

- Classical interpretation:

  normalization of Ψ_{SWF} coincides with the configurational partition function of a classical system of suitable flexible triatomic molecules

Previous discussion can be extended to this classical molecular solid

⇒ Ψ_{SWF} describes a quantum solid with vacancies and BEC

Computation of $\overline{X}_v$ for SWF:

at melting $\overline{X}_v$ = 1.4(1)x10^{-3}

- With $m^*=0.35m_{He}$ $T_{BEC}=11.3(X_v)^{2/3}\approx 0.14$ K
- $X_v(\tau)$ computed with SPIGS as $\tau\rightarrow\infty$?

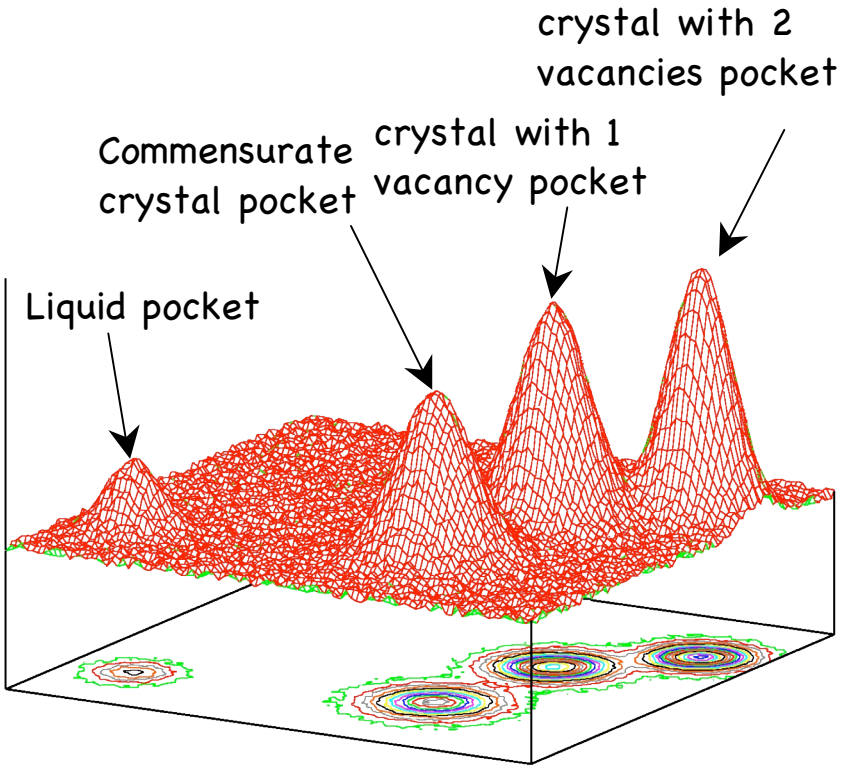

Properties at grain boundaries

Grain boundary obtained by rotation inside the basal plane by $\theta \approx 13°$

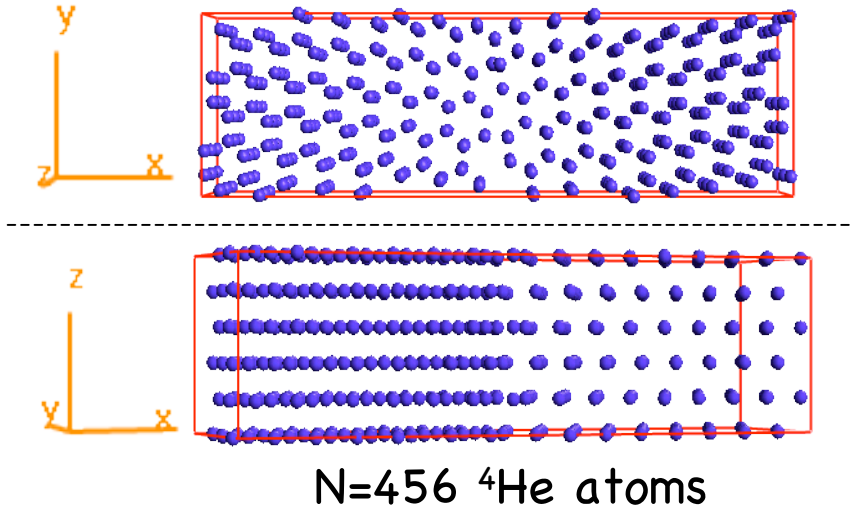

N=456 ^{4}He atoms

Intergrain width $\sigma \approx 9$ Å

Preliminary results: $\tau = 0.125\ K^{-1}$

Grain boundaries has high mobility

Study of correlations:

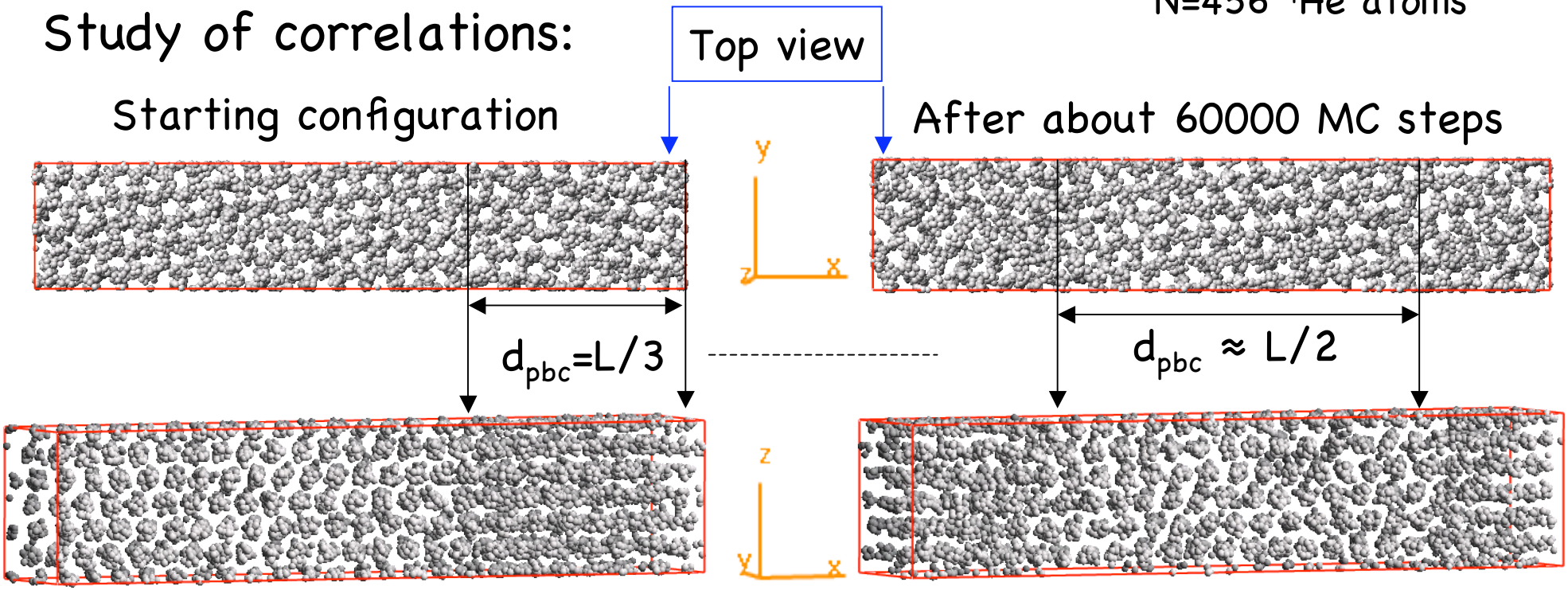

Evidence of coherent recrystallization waves

Properties at grain boundaries

Grain boundary obtained by rotation inside the basal plane by $\theta \approx 13°$

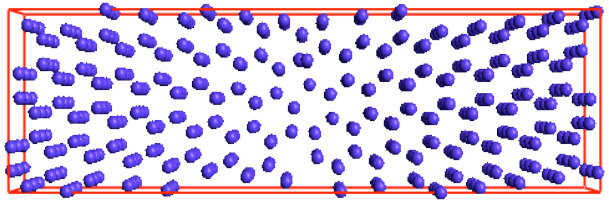

Interfacial energy: $E_I = \frac{E_{GB} - E_C}{2A}$

E_{GB}: energy system with grains
E_c: energy commensurate system

ρ (Å^{-3})	P (bars)	E_I (KÅ^{-2})	E_I + 1 vac.(KÅ^{-2})	E_I + 2 vac.(KÅ^{-2})	E_I + 4 vac.(KÅ^{-2})
0.0303	40	0.269±0.008	0.244±0.006	-	-
0.0313	54	0.305±0.004	0.283±0.004	0.250±0.005	-
0.0333	88	0.406±0.008	0.366±0.008	0.325±0.008	-
0.0353	142	0.546±0.005	0.482±0.006	0.418±0.005	0.261±0.005

- at the lowest density $E_I < 2\ E_{LC}$ being E_{LC} the liquid-crystal surface energy -> stability at phase coexistence
- Vacancies are easily adsorbed into the grain boundaries, relaxing the mechanical stress

Off-diagonal properties at grain boundaries

Top view; N=912 ^{4}He atoms

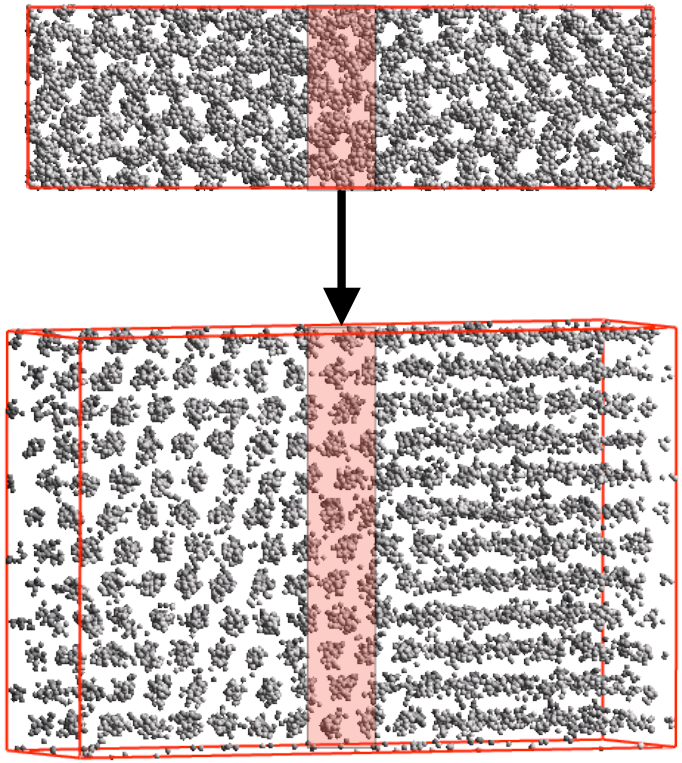

ρ=0.0313 Å^{-3}

Preliminary results: τ=0.125 K^{-1}

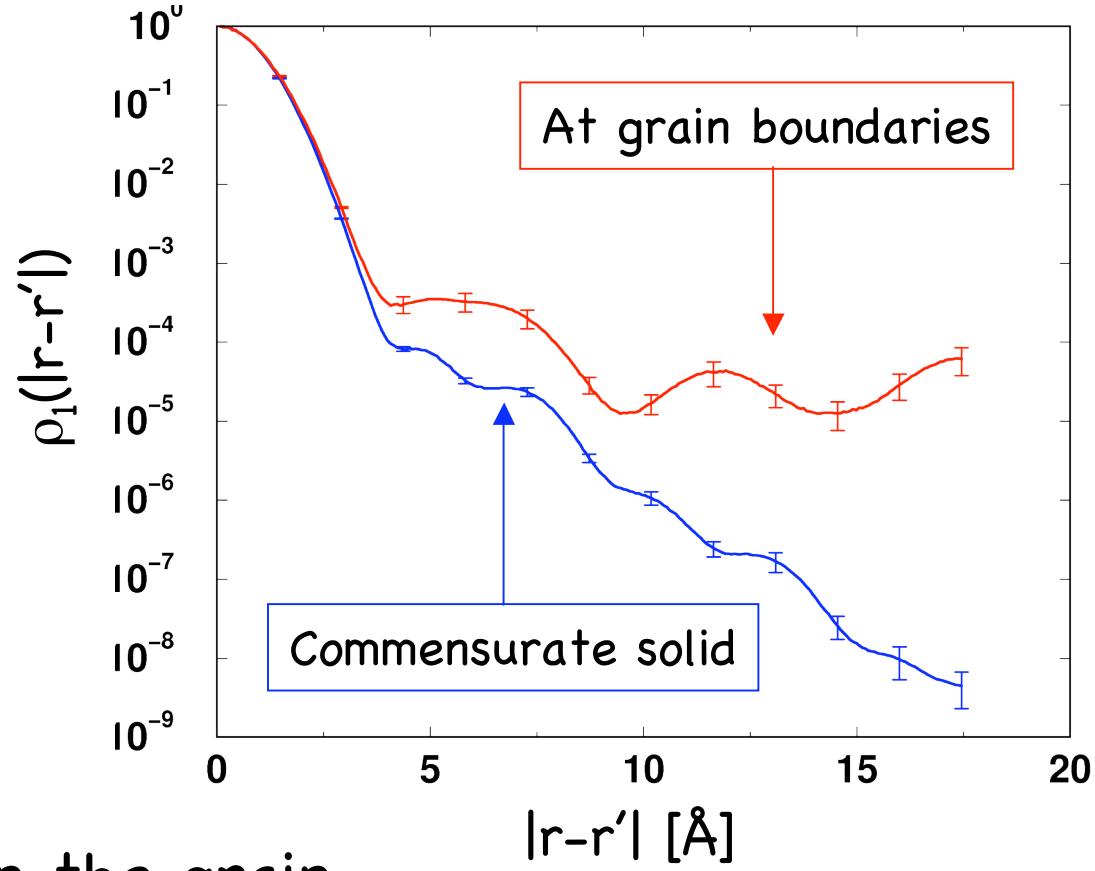

One body density matrix in the grain boundary: ODLRO is present, n_0=2.8 10^{-5}

Conclusions

Our main results for hcp ^{4}He at T=0 K

A. Is the ground state of **bulk** solid ^{4}He commensurate or incommensurate?
   - The best variational wave function (SWF) gives an incommensurate state, with X_v = 0.14 ± 0.01 % at melting

B. Multiple vacancies **do not** form a bound state

   in disagreement with PIMC results

C. ODLRO-BEC in the incommensurate solid
   - BEC is present, for the "exact" ground state $n_0 \approx 0.14$ per vacancy at the melting density

D. ODLRO-BEC in the commensurate solid
   - "Exact" ground state path integral (SPIGS): at present we can only give a (very low) upper bound: $n_0 < 2.5\ 10^{-8}$ at melting
   - In 2D evidence for exponential decay of the one-body density matrix

E. ODLRO-BEC in a grain boundary

   preliminary results indicate that high symmetry grain boundary has a finite n_0

   Evidence of coherent recrystallization waves

SWF & SPIGS: test on long-range contributions

- Zero-point motion of long-wavelength phonons induces in the wave function long-range r^{-2} correlations
(Reatto, Chester, Phys.Rev. 155, 1967)

We have performed two SPIGS computations, one starting from a SWF with the long range r^{-2} tail and one starting from a SWF without this long range.
Both SPIGS computations converge to the same result.

- Small effect on the ODLRO in the commensurate solid (fcc, ρ=0.029 Å^{-3}):
n_0=(2.5±1.0)x10^{-6} (SWF no long-range)
n_0=(4.1±1.4)x10^{-6} (SWF)

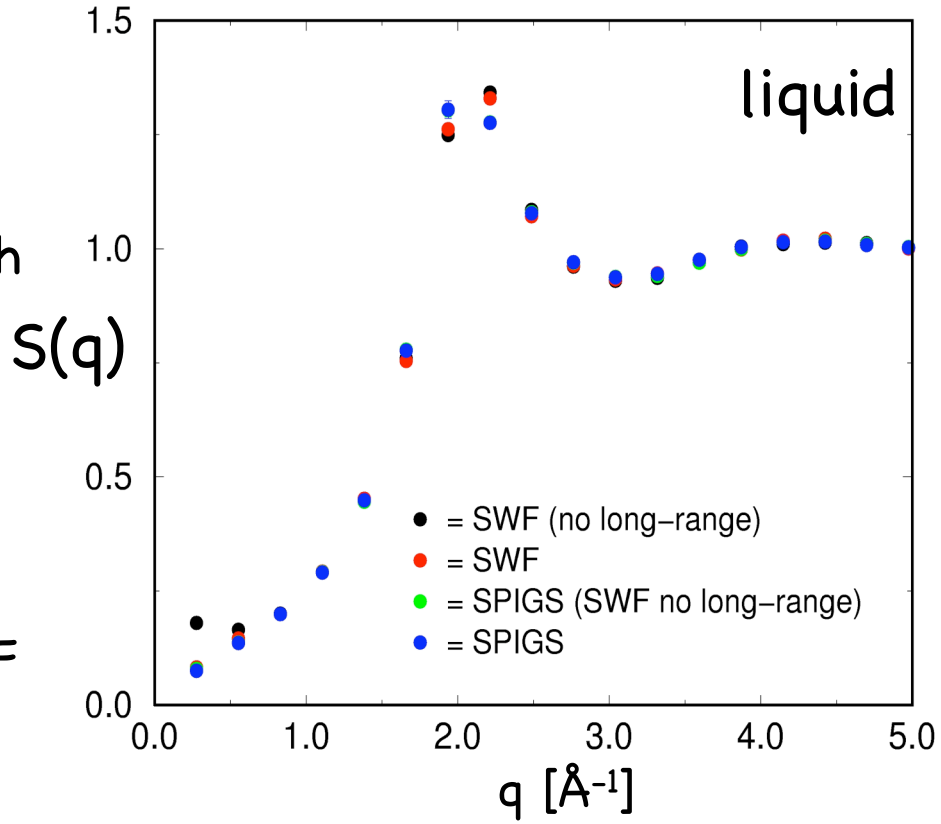

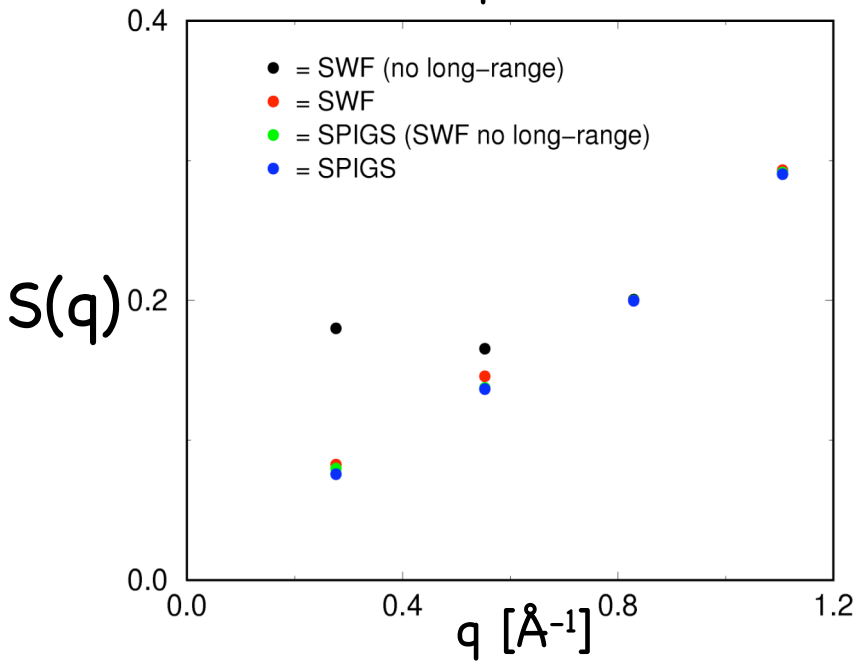

- Ground state energy per particle of a truly macroscopic system: $e_G=E_G/\mathcal{N}$
- Energy per particle from the simulation of a commensurate state: $e_0=E_0/N$
- Total energy from the simulation of an incommensurate state with one vacancy: $E_1=E_0+\Delta e_v$
- Estimated ground state energy per particle for the macroscopic system

$$e_G=e_0+X_v\Delta e_v$$

where X_v is the average concentration of vacancies as computed from $Q_{\mathcal{N}}$

- At melting the best energy of a wave function with localizing factors is 0.056 K per atom above SWF

$\Rightarrow$ allowing for $X_v\Delta e_v$, SWF are still the best for any $X_v<0.8\%$ ($\Delta e_v\approx 7$K at fixed lattice parameter)

How to compute the vacancy concentration in MC simulations

- The concentration of point defects in a quantum solid can be computed exploiting the well known quantum-classical isomorphism
  [J.A. Hodgdon and F.H. Stillinger, J. Stat. Phys. **78**, 117 (1995)]

- The concentration of vacancies in a classical solid can be obtained by a thermodynamic analysis of the extended system in the grand canonical ensamble and it is given by

$$x_v = e^{-\beta(\mu - f_1)}$$

  where μ is the chemical potential, f_1 is the activation energy of the defect (computed at fixed lattice spacing) and $\beta = 1/k_B T$
  [S.Pronk and D. Frenkel, J. Chem. Phys. **105**, 6722 (2001)]

- f_1 and μ can be computed in a standard canonical MC simulation adapting the Frenkel-Ladd method [D. Frenkel and A.J.C. Ladd, J. Chem. Phys. **81**, 3188 (1984); J.M. Polson, E. Trizac, S. Pronk and D. Frenkel, J. Chem. Phys. **112**, 5339 (2000)] to compute the free energy of a polymeric solid. This method is a particular case of Thermodynamic Integration in which the reference state is an Einstein crystal and the thermodynamic parameter involved is a coupling parameter artificially introduced.

Our variational tool: Shadow Wave Function

Evolution of Vitiello, Runge and Kalos, Phys. Rev. Lett. 60, 1970 ('88)

Ψ Includes many particle correlations via coupling to subsidiary variables

$$\Psi(R) = \phi_r(R) \times \int dS\, K(R,S) \times \phi_s(S)$$

Direct explicit Jastrow correlations

Indirect coupling via subsidiary (shadow) variables

Particles coordinates $R = \{\vec{r}_1, .., \vec{r}_N\}$

Shadow variables $S = \{\vec{s}_1, .., \vec{s}_N\}$

Jastrow terms: $\phi_r(R), \phi_s(S)$ $\quad K(R,S) = \prod_i^N e^{-C\left|\vec{r}_i - \vec{s}_i\right|^2}$

SWF functional form

- The SWF functional form can be interpreted as a first projection step in imaginary time of a Jastrow trial wave function ψ_J with a propagator G in the primitive approximation:

$$\Psi(R) = \int dS\, G(R,S) \times \psi_J(S)$$

$$R = \{\vec{r}_1,..,\vec{r}_N\}$$
$$S = \{\vec{s}_1,..,\vec{s}_N\}$$

$$= \int dS \prod_{i<j}^{N} e^{-u_r\left(|\vec{r}_i-\vec{r}_j|\right)} \prod_{i=1}^{N} e^{-C|\vec{r}_i-\vec{s}_i|^2} \prod_{i<j}^{N} e^{-u_r\left(|\vec{s}_i-\vec{s}_j|\right)} \times \prod_{i<j}^{N} e^{-u_J\left(|\vec{s}_i-\vec{s}_j|\right)}$$

$$= \int dS \underbrace{\prod_{i<j}^{N} e^{-u_r\left(|\vec{r}_i-\vec{r}_j|\right)}}_{\phi_r(R)} \underbrace{\prod_{i=1}^{N} e^{-C|\vec{r}_i-\vec{s}_i|^2}}_{K(R,S)} \underbrace{\prod_{i<j}^{N} e^{-u_s\left(|\vec{s}_i-\vec{s}_j|\right)}}_{\phi_s(S)} = \Psi^{SWF}(R)$$

The whole functional form is variationally optimized

SWF technique

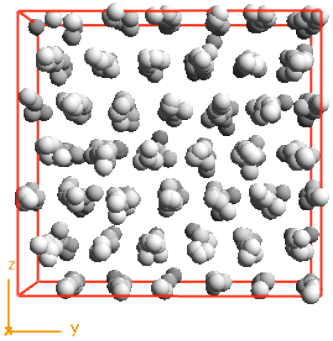

- Expectation value of a diagonal operator:

$$\frac{\left\langle \Psi^{SWF} \middle| \hat{O} \middle| \Psi^{SWF} \right\rangle}{\left\langle \Psi^{SWF} \middle| \Psi^{SWF} \right\rangle} = \int dR\, dS\, dS'\, \hat{O}(R) \frac{\phi_r^2(R) K(R,S) K(R,S') \phi_s(S) \phi_s(S')}{\left\langle \Psi^{SWF} \middle| \Psi^{SWF} \right\rangle}$$

$$p(R,S,S')$$

probability density in the extended space $\{R,S,S'\}$

$\Rightarrow$ 3N particles

- Integrals (over subsidiary and real variables) are computed with Metropolis Monte Carlo
- Equivalent to a canonical average for a classical system of special interacting flexible tri-atomic molecules:

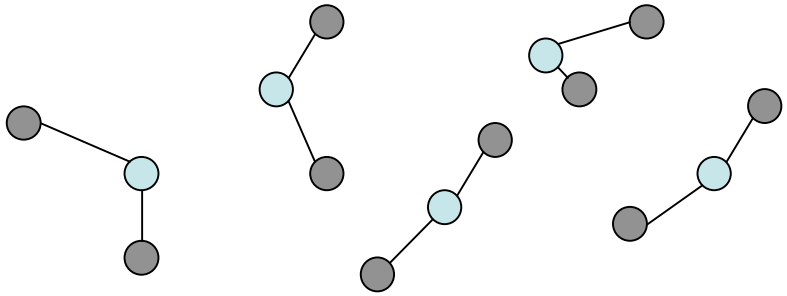

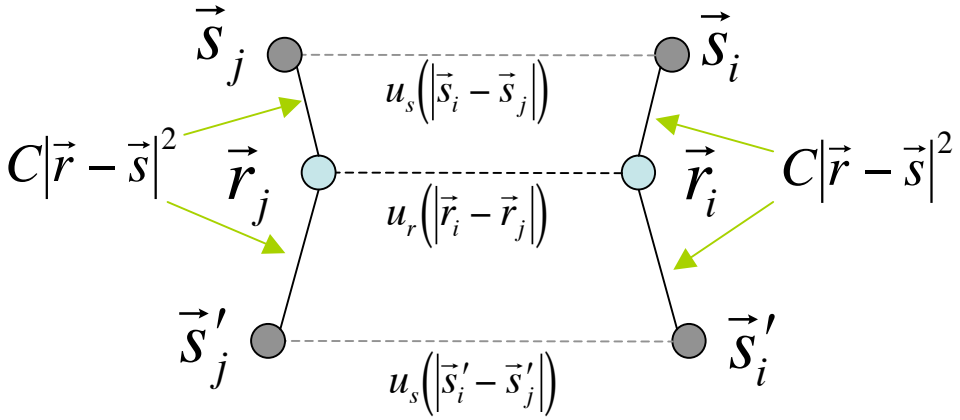

Imaginary short-time propagators

- Primitive: $\left\langle R\left|e^{-\delta\tau(\hat{T}+\hat{V})}\right|R'\right\rangle \cong \left\langle R\left|e^{-\frac{\delta\tau}{2}\hat{V}}e^{-\delta\tau\hat{T}}e^{-\frac{\delta\tau}{2}\hat{V}}\right|R'\right\rangle$

(bad for ^{4}He)

$$\cong e^{-\frac{\delta\tau}{2}V(R)}\prod_{i=1}^{N}\frac{e^{-\frac{|\vec{r}_i-\vec{r}_i'|^2}{4\lambda\delta\tau}}}{(4\pi\lambda\delta\tau)^{\frac{3}{2}}}e^{-\frac{\delta\tau}{2}V(R')}$$

Accurate up to terms of order $\delta\tau^2$: one assumes $\frac{\delta\tau^2}{2}\left[\hat{T},\hat{V}\right]=0$

With $V(R)=\sum_{i<j}^{N}v\left(\left|\vec{r}_i-\vec{r}_j\right|\right)$ (^{4}He)

and $\lambda=\frac{\hbar^2}{2m}$

- 4th order "Suzuki-Chin" (for ^{4}He accurate if $\delta\tau\approx10^{-3}$ K^{-1})

(Chin, Phys.Lett.A 226, 1997):

$$\left\langle R\left|e^{-\delta\tau(\hat{T}+\hat{V})}\right|R'\right\rangle \cong e^{-\delta\tau\left(\frac{2}{3}V(R)+\tilde{V}(R)\right)}\prod_{i=1}^{N}\frac{e^{-\frac{|\vec{r}_i-\vec{r}_i'|^2}{4\lambda\delta\tau}}}{(4\pi\lambda\delta\tau)^{\frac{3}{2}}}$$

$$\tilde{V}(R)=\begin{cases}0 & \text{if } R \text{ is "even"}\\ \frac{2}{3}V(R)+\frac{2\lambda\delta\tau^2}{9}\sum_{i=1}^{N}\left(\vec{\nabla}_i V(R)\right)^2 & \text{elsewhere}\end{cases}$$

- Pair-product (for ^{4}He accurate when $\delta\tau\approx10^{-2}$ K^{-1})

(for a review Ceperely, Rev.Mod.Phys. 67, 1995):

$$\left\langle R\left|e^{-\delta\tau(\hat{T}+\hat{V})}\right|R'\right\rangle \cong G(R,R',\delta\tau)=\prod_{i<j}^{N}e^{-u(\vec{r}_i-\vec{r}_j,\vec{r}_i'-\vec{r}_j',\delta\tau)}\prod_{i=1}^{N}\frac{e^{-\frac{|\vec{r}_i-\vec{r}_i'|^2}{4\lambda\delta\tau}}}{(4\pi\lambda\delta\tau)^{\frac{3}{2}}}$$

where $u(\vec{r},\vec{r}',\delta\tau)$ is obtained by imposing that $G(R,R',\delta\tau)$ is exact for N=2

The SPIGS method

Galli, Reatto, Mol. Phys. 101, 2003

- Correlations:

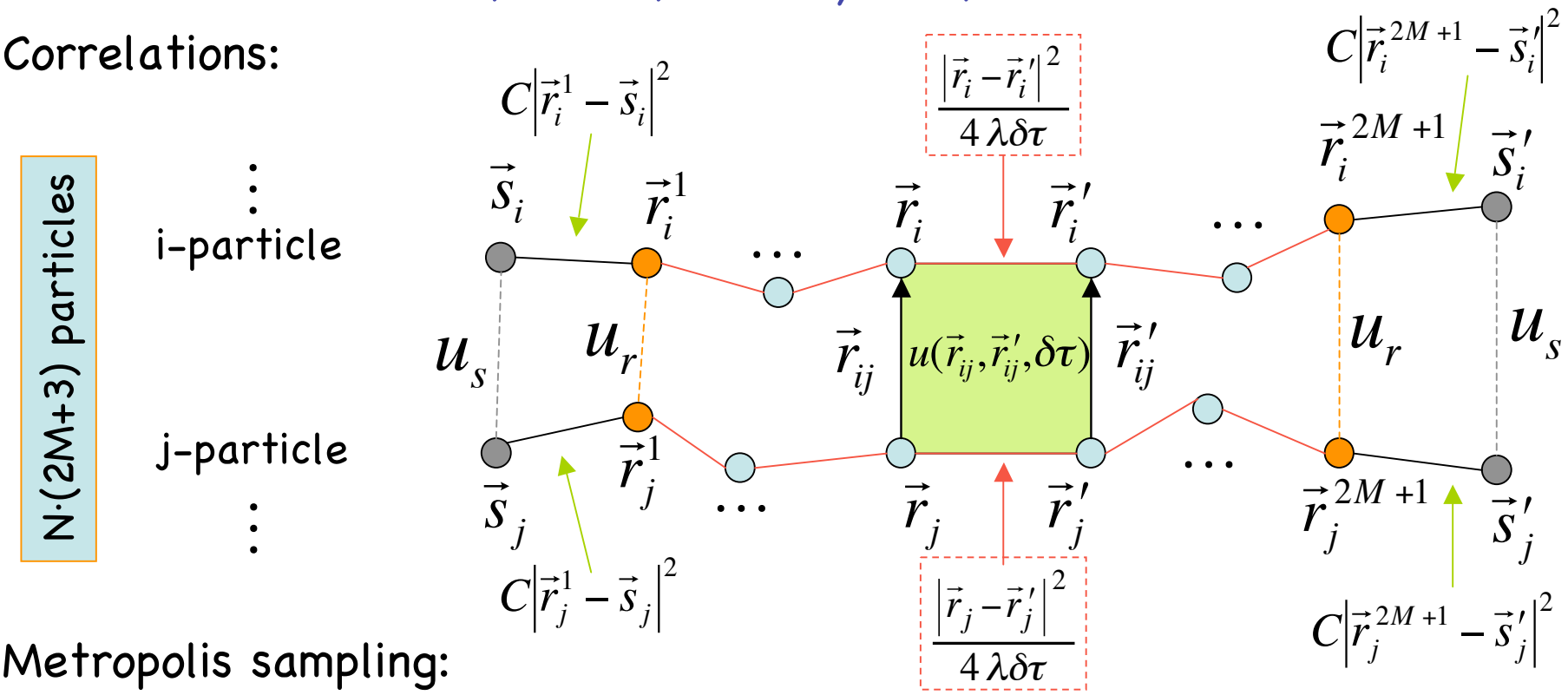

- Metropolis sampling:
  - Multilevel moves: bisection
  - Rigid translation of the polymers
  - Single particle moves
  - Sampling of permutation is not necessary:

  SWF is Bose-symmetric
  - Verlet neighbour list

Commensurate crystal
SWF results: ODLRO in a basal plane

- We have computed the one-body density matrix in a basal plane of an hcp solid and along a single axis (n.n. direction)
- ODLRO is present and it is anisotropic only in the middle range 3-14 Å
- Good agreement with the result obtained by sampling in one dimension (n.n. direction)

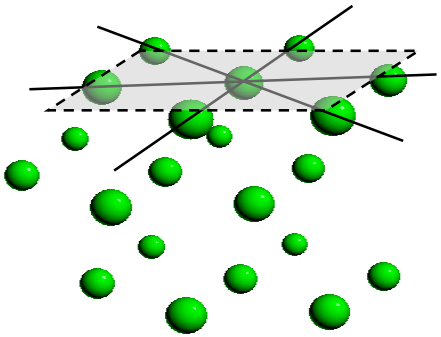

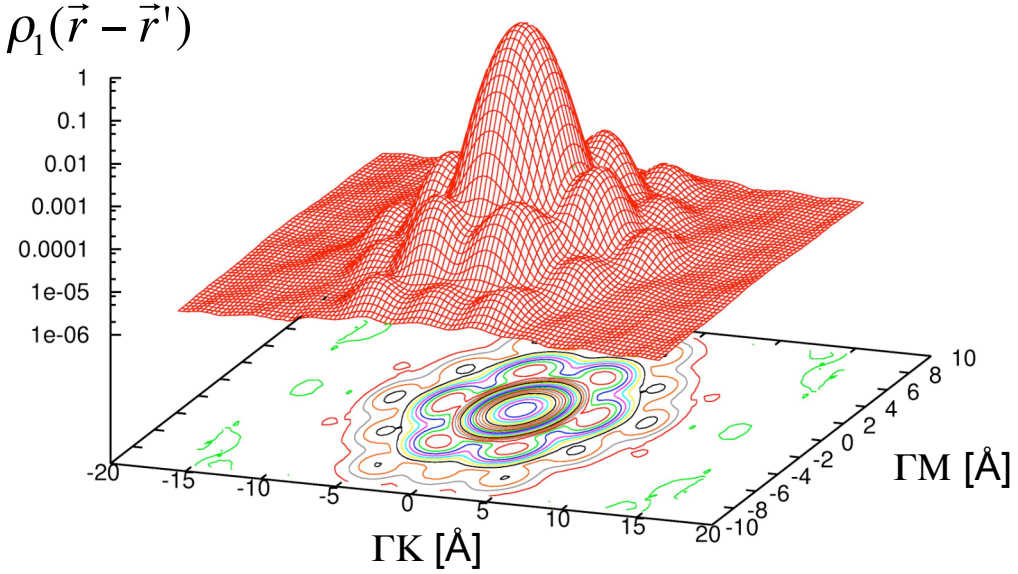

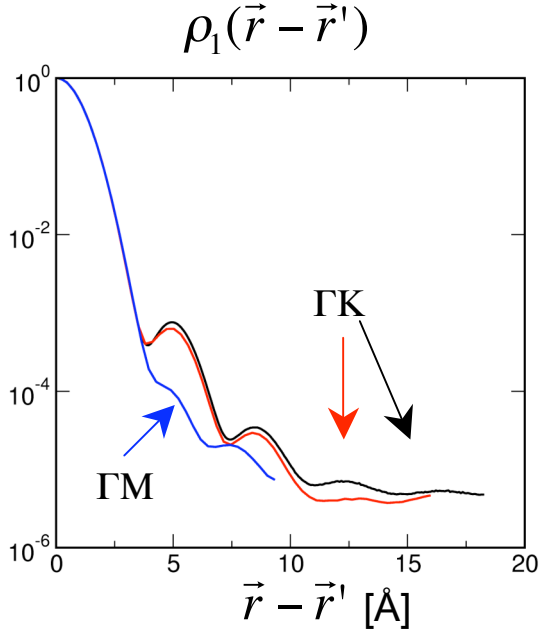

PIGS versus SPIGS

- Imaginary time evolution from different trial wave function: expectation value of the energy

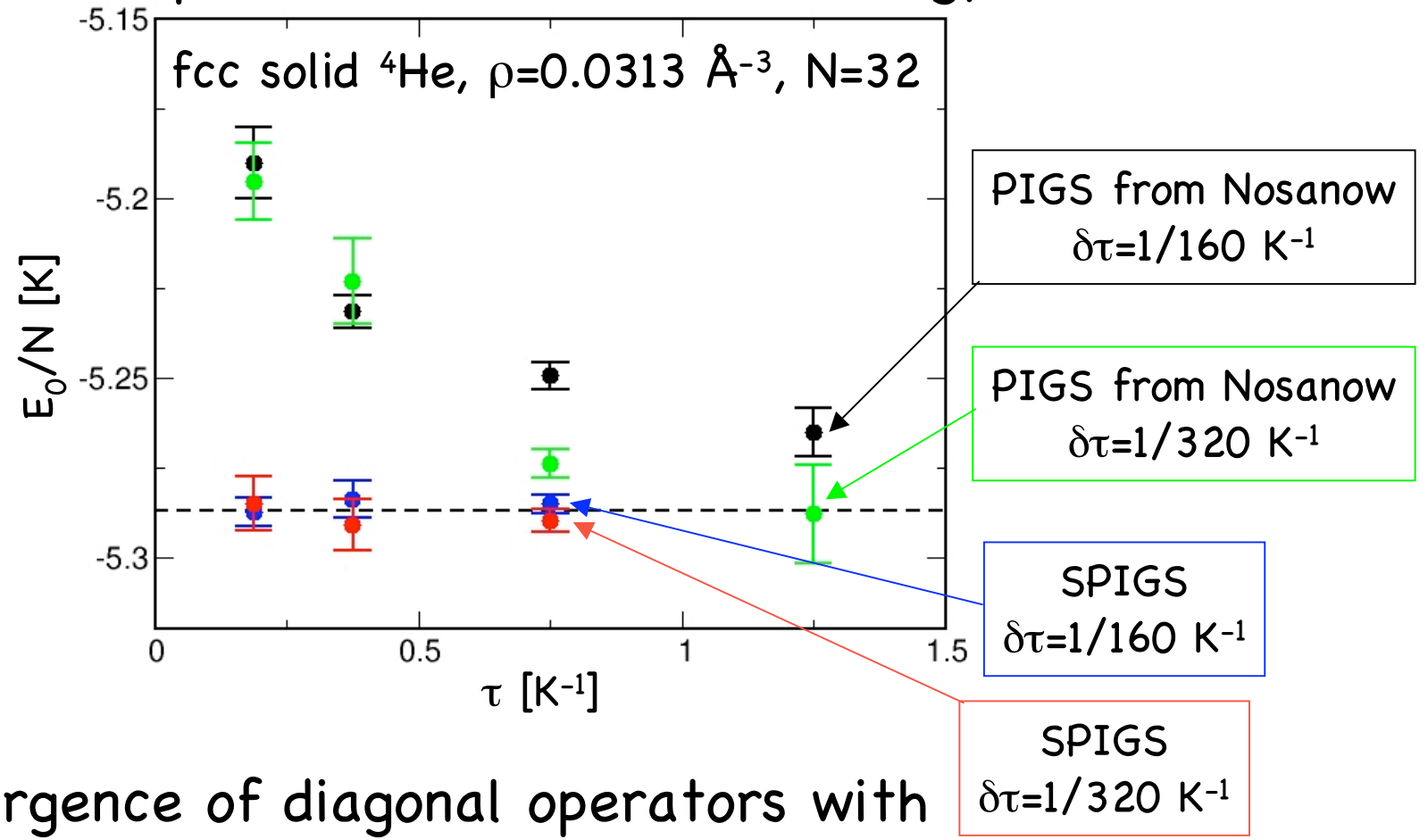

- Convergence of diagonal operators with both wave functions is already obtained at τ=0.2 K^{-1}